POLITECNICO DI TORINO
Repository ISTITUZIONALE

ZnO micro- and nano-structures for the design of piezoelectric composites: recent advances in energy harvesting applications

Original
ZnO micro- and nano-structures for the design of piezoelectric composites: recent advances in energy harvesting applications / Duraccio, D., Malucelli, G.. - In: DISCOVER MATERIALS. - ISSN 2730-7727. - ELETTRONICO. - 6:(2026), pp. 1-30. [10.1007/s43939-025-00460-y]

Availability:
This version is available at: 11583/3007207 since: 2026-02-02T16:40:15Z

Publisher:
Springer

Published
DOI:10.1007/s43939-025-00460-y

Terms of use:

This article is made available under terms and conditions as specified in the corresponding bibliographic description in the repository

Publisher copyright

(Article begins on next page)

19 November 2026

Discover Materials

REVIEW

Open Access

ZnO micro- and nano-structures for the design of piezoelectric composites: recent advances in energy harvesting applications

Donatella Duraccio[1*] and Giulio Malucelli[2,3]

*Correspondence:
Donatella Duraccio
donatella.duraccio@stems.cnr.it
[1]Institute of Sciences and Technologies for Sustainable Energy and Mobility, National Council of Research, Strada delle cacce 73, 10135 Turin, Italy
[2]Department of Applied Science and Technology, Politecnico Di Torino, Viale T. Michel 5, 15121 Alessandria, Italy
[3]Consorzio Interuniversitario Nazionale Per La Scienza E Tecnologia Dei Materiali (INSTM), Via G. Giusti 9, 50121 Florence, Italy

Abstract

One of the current world's challenging issues concerns the design, development, and exploitation of efficient devices for energy harvesting that, in the last few years, has gathered a growing interest not only from academia but also from an industrial point of view. Although the general concept of (macro)energy harvesting has been successfully exploited for centuries in the design of passive solar power systems, as well as wind and water mills, only during the last 10 to 15 years there has been particular attention toward the development of effective (micro)energy harvesting systems, exploiting the energy from the ambient provided by light, radiofrequency radiation, or motion/vibration/thermal sources. These (micro)energy harvesting systems require efficient and reliable materials to convert the input environmental energy into an exploitable electrical output. In this context, among the most currently employed ceramics, zinc oxide (ZnO), both micro- and nano-structured, is gaining more and more importance in the design of energy harvesting devices because of its interesting features that comprise low cost, high piezoelectric characteristics, and ease of production, among others. The present work aims to summarize the current state-of-the-art on the use of ZnO micro- and nano-structures for the design and manufacturing of advanced piezoelectric devices and to provide the reader with some recent progress that may pave the way toward further advances in the forthcoming years.

Keywords Energy harvesting, ZnO, Piezoelectric behaviour, Bulk piezoceramic ZnO systems, Polymer-ZnO piezoelectric systems

1 Introduction

The energy harvesting (or scavenging) concept stems from the current wide use of electronic battery-powered devices, which can also be wearable and implantable. Some common battery-powered devices are presented in Fig. 1, together with their average power consumption and energy autonomy. In particular, these applications usually require lightweight, compact, and low-cost energy sources, which ensure the desired manageability and energy autonomy [1].

© The Author(s) 2026. **Open Access** This article is licensed under a Creative Commons Attribution-NonCommercial-NoDerivatives 4.0 International License, which permits any non-commercial use, sharing, distribution and reproduction in any medium or format, as long as you give appropriate credit to the original author(s) and the source, provide a link to the Creative Commons licence, and indicate if you modified the licensed material. You do not have permission under this licence to share adapted material derived from this article or parts of it. The images or other third party material in this article are included in the article's Creative Commons licence, unless indicated otherwise in a credit line to the material. If material is not included in the article's Creative Commons licence and your intended use is not permitted by statutory regulation or exceeds the permitted use, you will need to obtain permission directly from the copyright holder. To view a copy of this licence, visit http://creativecommons.org/licenses/by-nc-nd/4.0/.

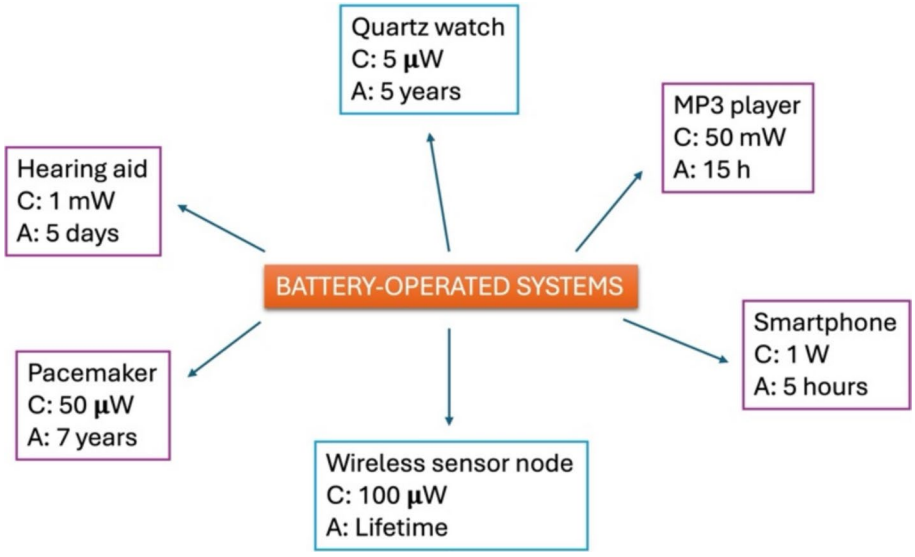


Fig. 1 Some current common battery power devices. Legend: C = average energy consumption; A = energy autonomy

However, despite the significant improvements of the batteries currently employed, the impact in terms of size, costs, and sustainability has pushed both academia and the industrial world toward the seeking of suitable reliable alternatives that comprise: i) the substitution of batteries with miniaturized fuel cells [2], which possess higher energy density; ii) the delivery of the needed energy to devices through wireless modes (this strategy has already been exploited for Radio Frequency Identification (RFID) tags, despite some issues regarding the need of specific transmission infrastructures [3]; iii) the harvesting of the ambient energy (vibrational, thermal, motion energy, RF radiation, or light). This last strategy can exploit electrostatic, electromagnetic, or piezoelectric mechanisms for converting motion/vibration energy into electrical energy, generating from micro- to milliwatts of power based on the ambient conditions [4–6]. In particular, piezoelectric conversion of motion/vibration is gaining increasing interest because of the ease of processing, the high conversion efficiency, and the wide availability of effective piezoelectric materials [7–9].

From a general point of view, in a piezoelectric transducer, movement or vibrations promote the deformation of a piezoelectric capacitor, hence producing a voltage that can be stored and used on demand. This effect can be achieved by employing three main piezoelectric materials, i.e., piezopolymers, polymer matrix-based piezocomposites, and piezoceramics. At present, piezoceramics are preferred as they account for high energy conversion rates and remarkable electro-mechanical coupling constants. However, looking at the most currently employed piezoceramics, PZT (lead zirconate titanate) shows some environmental problems due to the toxicity of lead [10], while $BaTiO_3$ (barium titanate), despite interesting piezoelectric features, shows some limitations concerning its low Curie temperature (not exceeding 160 °C [11]), which restricts the envisaged technological applications. Additionally, aluminium nitride (AlN) has a relatively low piezoelectric coefficient, resulting in limited energy harvesting efficiency and low output voltage; it is also brittle, making it unsuitable for flexible or stretchable applications unless used as a thin film [12]. Besides, such a polymer as PVDF needs poling, its piezoelectric output is relatively low, and it has limited thermal stability (up to ~ 150 °C) [13].

Conversely, ZnO is emerging as an effective piezoelectric material, as it is a lead-free and low-cost material, it can be synthesized in different structures (microspheres, short and long needles, flowers, bi-pyramids, nanorods, nanotetrapods…), and can be employed both as piezoelectric bulk material and in the form of film, even as a piezo-filler in polymer matrices that do not exhibit any piezoelectric feature [14–18]. Table 1 collects the key properties of ZnO alongside other prominent piezoelectric materials [19–22].

The current interest in ZnO as a piezoceramic material is well evidenced by the increasing number of scientific articles that have appeared in the literature to date (Fig. 2).

Despite the huge number of reviews in the scientific literature on piezoelectric systems for energy harvesting, most of them are not specifically focused on ZnO but discuss the piezoelectric behavior of different materials (also including zinc oxide) [22–37]. Furthermore, some notable papers that specifically address the piezoelectric properties of ZnO are not up to date [38–42].

Therefore, this review aims to provide readers with an up-to-date overview of the use of ZnO as an effective piezoelectric material for energy harvesting. First, we will describe its structure and synthesis methods. Then, we will summarize some of ZnO's main properties, focusing specifically on its piezoelectric behavior. Lastly, we will discuss

Table 1 Key properties of main piezoelectric materials for energy harvesting

Property	ZnO	$BaTiO_3$	PZT	AlN	PVDF
Material Type	Inorganic semiconductor	Inorganic ferroelectric	Inorganic ferroelectric ceramic	Inorganic nitride semiconductor	Ferro-electric polymer
Typical Output Voltage (V)	Moderate (~0.1–5)	Moderate–High (~1–10)	High (~1–20)	Low (~0.1–1)	Low–Moderate (~0.1–5)
Energy Conversion Efficiency	Moderate	High	Very high	Low–moderate	Low–moderate
Piezoelectric Coefficient (d_{33}) (pC/N)	~10–15	~190	~200–600	~5	~20–30 pC/N
Poling Requirement	Not required	Required	Required	Not required	Required
Thermal Stability	Moderate (up to ~300 °C)	Moderate (~130 °C Curie temperature)	High (~350 °C Curie temperature)	Very high (> 600 °C)	Limited (~100–150 °C)
Chemical/Environmental Stability	Moderate (sensitive to moisture/UV)	Moderate	High	Excellent	Moderate
Flexibility	Low	Low	Very low	Low	High
CMOS* Compatibility	Moderate	Poor	Poor	Excellent	Moderate
Fabrication Ease	Easy (low-temp methods, solution processing)	Moderate	Difficult (sintering, high-temp)	High (thin-film deposition)	Very easy (solution processing)
Integration in Flexible Systems	Good (composites with polymers)	Limited	Limited	Moderate	Excellent
Typical Forms for Energy Harvesting	Nanowires, nanorods, thin films, composites	Ceramics, films	Bulk ceramics, thick/thin films	Thin films (MEMS/NEMS)	Films, electrospun fibers, composites

* CMOS = Complementary Metal-Oxide Semiconductor

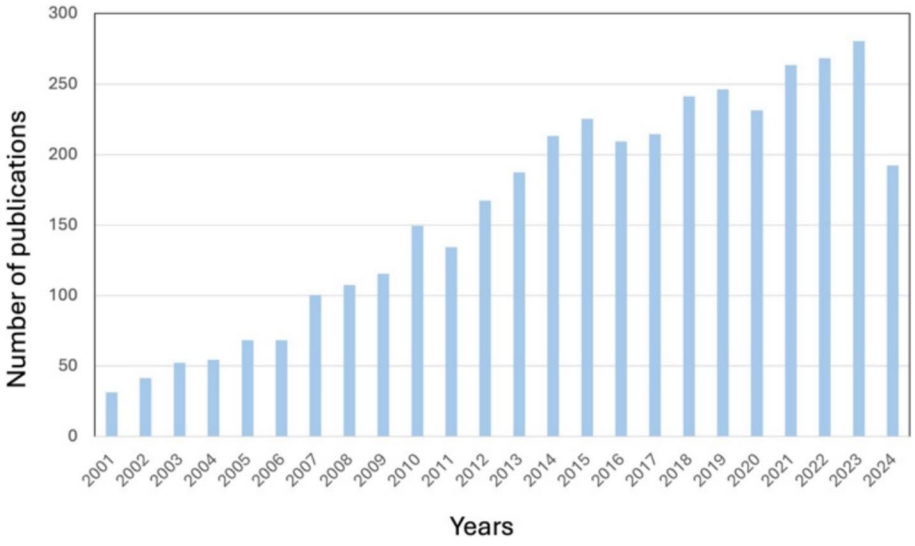


Fig. 2 The number of publications (from 2001 to 2024) in peer-reviewed journals, dealing with "ZnO AND Piezoelectric" (AND is the Boolean operator; data collected from the Web of Science.™ database, www.webofscience.com, accessed on 14 October 2024)

some recent applications of this piezoelectric ceramic embedded in a polymer matrix or grown on a selected substrate as a crystal with specific morphology and orientation. We will highlight the current limitations and challenges and discuss possible research trends for the coming years.

2 Structure, properties, and morphology of ZnO

Although ZnO typically crystallizes in the hexagonal wurtzite structure, it can also exist in cubic zincblende or rocksalt forms under certain conditions [4] (Fig. 3). At ambient temperature and pressure, wurtzite is the thermodynamically stable form of ZnO [7]. It belongs to the space group of P6 3mc and is characterized by a ratio of the lattice constants *c/a* similar to the ideal value of a hexagonal cell (i.e., 1.633) [10]. Zincblende ZnO is stable only when grown on a substrate with a cubic lattice structure. From a crystallographic point of view, the zincblende and wurtzite structures share a similar atomic arrangement, with the main distinction being the orientation of adjacent tetrahedral units. In the zincblende structure, the angle between these units is 60°, whereas in the wurtzite phase, it is 0°. This difference in angular configuration results in distinct crystal symmetry and lattice properties for each phase [11]. In addition to these polymorphs, ZnO can crystallize in the rocksalt form when the pressure increases above 10 GPa [14], with the transition pressure depending on both temperature and grain size [4]. The high bond polarity of ZnO makes the wurtzite more stable than the zincblende structure [15].

ZnO is a white, powdery material at room temperature and has a variety of unique properties that make it valuable in many fields as resumed in Table 2 [43–45]. Among them, it is worth highlighting that ZnO is an II-VI semiconductor with a direct wide band gap ($E_G = 3.37$ eV [16, 17]) and is ideal for ultraviolet (UV) and blue wavelength optoelectronic applications, due to its substantial exciton binding energy (60 meV [46]). Its refractive index, as low as 2.05 [47, 48], leads to better light coupling, enhanced emission efficiency, and reduced optical losses, making it particularly beneficial for such

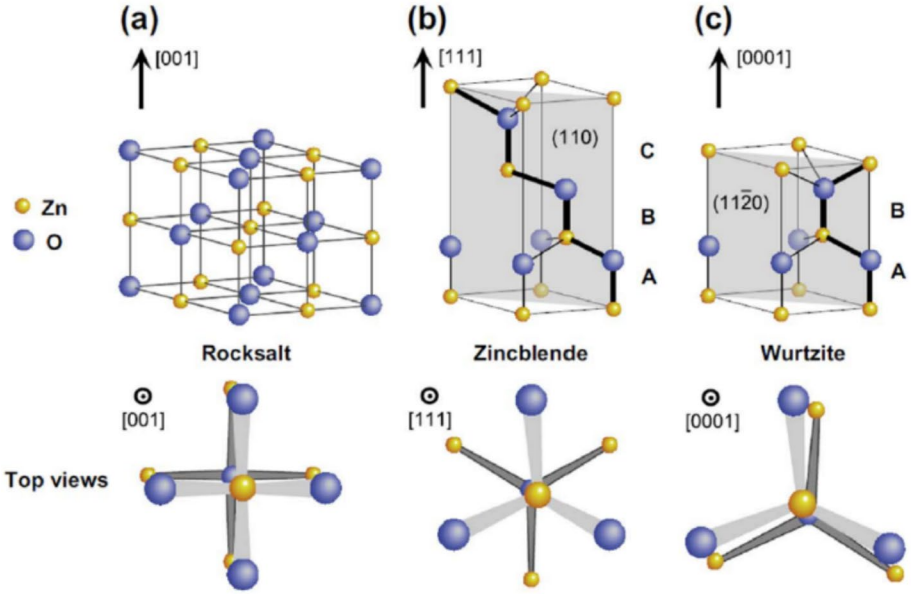


Fig. 3 ZnO crystal structures represented by sticks and balls: cubic rocksalt (**a**), cubic zincblende (**b**), and hexagonal wurtzite (**c**). Reprinted with permission from [4].
Copyright Elsevier, 2020

Table 2 Main properties of ZnO

Appearance	**Amorphous white or yellowish white powder**
Density (g/cm^3)	5.606
Melting point (°C)	1975
Nature of oxide	Amphoteric species
Thermal conductivity (W/(mK)	0.6–1.2
Linear expansion coefficient (K^{-1})	2–6 × 10^{-6}
Bandgap at room temperature (eV)	3.37
Bandgap at 4 K (eV)	3.44
Relative dielectric constant	8.66
Refractive Index	2.04
Intrinsic carrier concentration (1/cm^3)	10^{16}–10^{20}
Exciton binding energy (meV)	60
Breakdown voltage (V/cm)	5.0 × 10^6
Electron Hall mobility at 300 K (cm^2/(V·s))	200
Hole Hall mobility at 300 K (cm^2/(V·s))	5–50
Ionicity (%)	62

devices as light-emitting diodes (LEDs) and laser diodes. ZnO has intrinsic antibacterial properties, making it useful in medical and cosmetic products [49, 50].

ZnO is thermally stable and can withstand high temperatures without decomposing; for these reasons, it is used as a catalyst in various chemical reactions [51–53]. Also, ZnO exhibits piezoelectricity due to its non-centrosymmetric wurtzite crystal structure, which allows it to generate an electric field in response to mechanical stress along the ZnO *c*-axis by shifting the positions of the centers of the positive Zn and negative O charges, thus altering the dipole moments within the crystal. This piezoelectric effect makes ZnO suitable for applications including pressure and strain sensors and mechanical energy harvesting from vibrations or motion [52, 54–57].

ZnO can be synthesized in various morphologies, each significantly influencing the electronic, optical, and catalytic properties, which makes them versatile for various technological applications [52]. Indeed, ZnO nanostructures can be classified into different dimensions based on their shape and size, namely: zero-dimensional (0D), one-dimensional (1D), two-dimensional (2D), and three-dimensional (3D) forms. 0D ZnO structures are nanoparticles or quantum dots with all three dimensions confined to the nanometer scale. They are usually spherical or nearly spherical, having a size range of a few nanometers; they can be employed in bio-imaging, drug delivery, and sensors, among others (Fig. 4A).

1D ZnO structures are elongated in one dimension, giving rise to the formation of nanorods, nanofibres, nanowires, nanobelts nanotubes nanohelixes, nanoribbons nanorings, and nanoneedles. As the other two dimensions are remarkably confined, these structures are provided with high aspect ratios [52, 53] (Figs. 4B-E). 1D ZnO has widespread potential application in electronics, field-effect transistors (FETs), gas sensors, and nanogenerators [58]. Conversely, 2D structures have two dimensions extended in a plane, with the third dimension being very thin, hence originating nanowhiskers, hexagonal, nanoplates, porous nanosheets, ultrathin nanosheets, nanoflakes, nanowalls, nanosheets or thin films. The large specific surface area and polar faces [59] possessed by 2D ZnO make ZnO nanosheets superior candidates not only for solar cells but also for photocatalysis: indeed, the large specific surface area of ZnO enables more contaminants to be adsorbed onto its active surface, thus leading to more pollutants being attacked by hydroxyl radicals.

Finally, 3D structures are complex architectures formed by the assembly of lower-dimensional units (0D, 1D, or 2D); they exhibit three extended dimensions and various morphologies like flowers, hierarchical structures, or mesoporous frameworks microspheres (Fig. 5). Due to larger surface-to-volume ratios and porosity, they can be employed in gas sensing and energy storage applications.

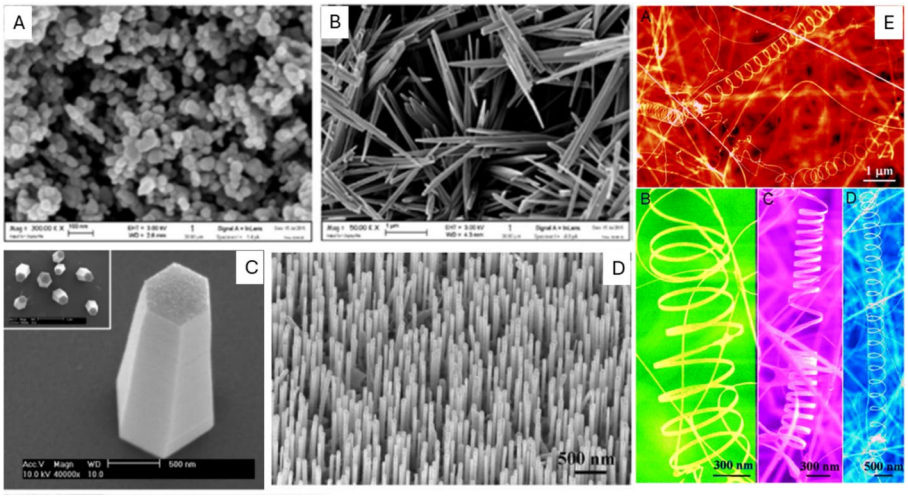


Fig. 4 Typical Scanning Electron Microscopy (SEM) images of (**A**) 0D ZnO nanospheres employed for the fabrication of microcantilevers. Reprinted with permission from [56].
Copyright Elsevier, 2017. (**B**) 1D ZnO needles. Reprinted with permission from [56]. Copyright Elsevier, 2017. (**C**) 1D ZnO nanorods. Reprinted with permission from [57]. Copyright ACS, 2006. (D) 1D ZnO nanowires, potentially suitable for the fabrication of nanogenerators. Reprinted with permission from [61]. Copyright Elsevier, 2009. (E) 1D ZnO nanobelts, suitable for the fabrication of 1-D nanoscale sensors, transducers, and resonators. Reprinted with permission from [60]. Copyright ACS, 2003

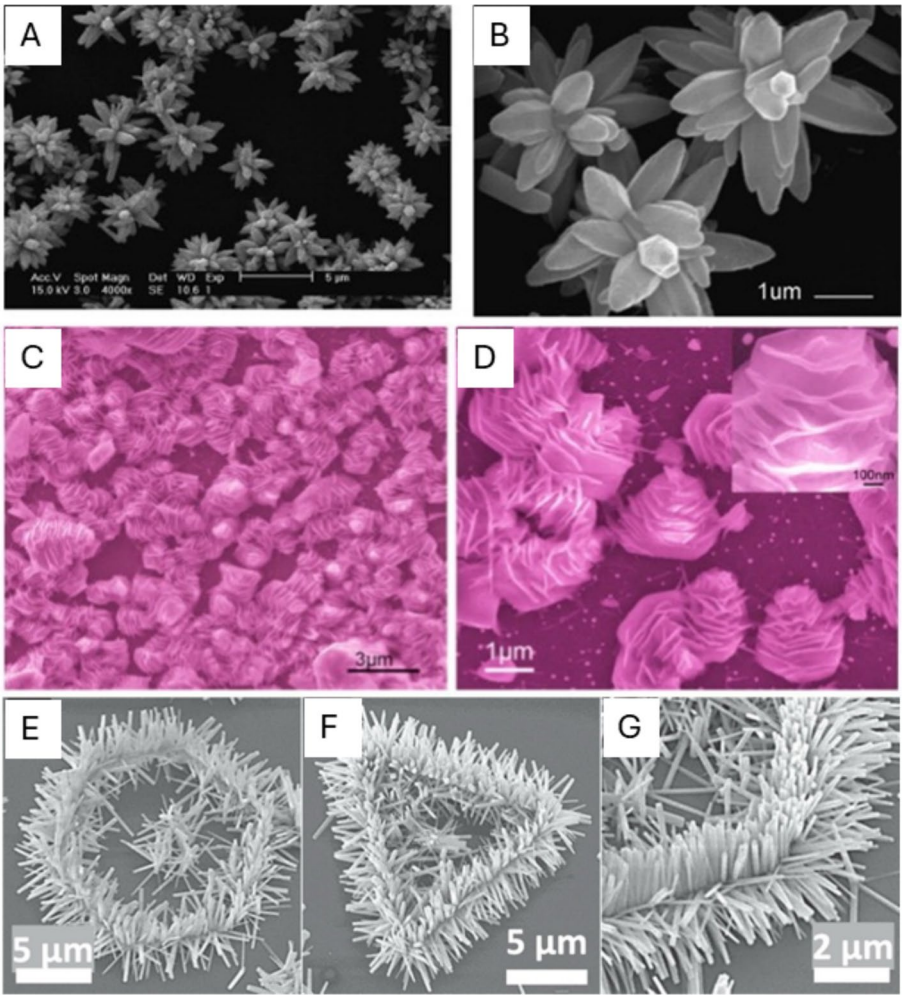


Fig. 5 (**A** and **B**) Typical field emission SEM (FESEM) images of various 3D flower-like ZnO structures at different magnifications. Reprinted with permission from [62].
Copyright Elsevier, 2007. (**C** and **D**) 3D structure of rose-like ZnO nanoflowers at different magnification. Reprinted with permission from [63]. Copyright Elsevier, 2009. (**E**–**G**) SEM image of ZnO hierarchical nanorings grown from hexagonal nanodisk (**E**) and from triangle nanodisk **(F)**; magnified SEM image showing the secondary ZnO nanowires (**G**). These nanorings are potentially suitable for the fabrication of electrodes for gas sensing. Reprinted with permission from [64]. Copyright Elsevier, 2018

3 Synthesis of ZnO micro- and nano-structures

ZnO can be synthesized through various techniques, utilizing both solution-based and vapor-phase approaches. Solution methods encompass sol–gel, microemulsion, precipitation/co-precipitation, hydrothermal, solvothermal, polyol, sonochemical, microwave-assisted, and electrospinning techniques [65]. Vapor phase preparation includes pulsed laser deposition [66], molecular beam epitaxy (MBE) [4], physical vapor deposition [67, 68], thermal evaporation [69], chemical vapor deposition [63, 70] (including metal–organic chemical vapor deposition (MOCVD) [71], and plasma enhanced chemical vapor deposition (PECVD) [72].

The most common approach for ZnO synthesis is the sol–gel method because of its low cost, simplicity, and relatively mild synthesis conditions ("soft chemistry") [73]. In addition, the nanoparticles' morphology can be tuned by controlling the reaction rate. The sol–gel method consists of a series of consecutive chemical steps, starting with

hydrolysis, followed by condensation, polymerization, and ending with the growth and aging of particles [74]. More in detail, a ZnO precursor is first dissolved in alcohol; then, an alkali solution (e.g., NaOH or NH_4OH) is added dropwise to the precursor solution under stirring. The solution is aged, leading to the formation of a gel that is dried and then calcined at high temperatures (300–500 °C) to form ZnO nanoparticles. Zn propoxide and acetate are the most employed precursors as they readily react with water and enhance the hydrolysis reaction [75]. Precursors, solvents, and additives used during the sol–gel synthesis of ZnO nanoparticles are thoroughly reviewed elsewhere [75].

As found in the scientific literature, selective control of the pH of the sol–gel solution alters the size and optical properties of ZnO nanoparticles [76]. Calcination and annealing temperature also play an essential role in tailoring the size, shape, and optical properties of the synthesized ZnO nanoparticles [77]. Capping agents/surfactants introduced as additives also affect the morphology of the synthesized oxide [76].

Similarly to the sol–gel process, such low-temperature wet chemical methods as hydrolysis, precipitation, and hydrothermal processes are cost-effective and scalable: they have been used to prepare a wide variety of ZnO nanostructures [78]. In a typical precipitation and co-precipitation reaction, a reducing agent (generally an inorganic alkali) reacts with a zinc salt. This produces a precipitate that is washed and calcined at a certain temperature, allowing to obtain particles with desired morphology and characteristics [79]. In solvothermal and hydrothermal processes, a zinc salt and a base (e.g., NaOH) are dissolved in hot solvents (other than water) or water, respectively, and transferred to an autoclave under high pressure (1–10.000 atm) and temperature (100–1000 °C). These methods are also useful for the synthesis of different metastable and thermodynamically stable ZnO structures through the tailoring of the reaction conditions [80, 81].

In the microemulsion method, micelles provide a well-defined nanoreactor environment offering precise control over the size, shape, and uniformity of the resulting ZnO nanoparticles [82–84]. The process involves the preparation of two microemulsions containing the same two immiscible liquids (usually oil and water) and a surfactant. One microemulsion includes Zn salt (i.e., Zn^{2+} ions), and the second a precipitating agent (usually a base like NaOH or NH_4OH). The emulsions are mixed under controlled conditions, and the reactants from the two water droplets diffuse and react inside the droplets. Zinc hydroxide is the first product formed inside the microdroplets and undergoes thermal decomposition by aging the solution, leading to the formation of ZnO nanoparticles inside the water droplets [82]. The resulting microemulsion is broken down by adding a polar solvent like ethanol or acetone, which separates ZnO nanoparticles from both surfactant and oil. ZnO nanoparticles are then collected by centrifugation or filtration. This method is often used when monodispersity is crucial, such as in optoelectronics, catalysis, or sensor technology: indeed, the microemulsion can effectively control the particle size and protect the nanoparticles from excess aggregation due to its "cage" effect. However, it requires careful optimization of the reaction conditions and is more suited for lab-scale production than large-scale industrial synthesis [82].

In the polyol method, ZnO is nucleated and grows in a high-boiling polyol like ethylene glycol, diethylene glycol, tetraethylene glycol, or glycerol. The polyol acts as a solvent and stabilizing agent that limits particle growth and suppresses particle agglomeration. Further, the synthesis is easy to perform and requires neither multi-sequential steps nor

advanced experimental conditions or equipment [85, 86]. Microwave-assisted [87, 88] and sonochemical synthesis [89] employ microwave radiation and ultrasonic waves, respectively, for the preparation of ZnO particles. The application of these waves to a zinc precursor and a base solution facilitates the formation of particles with a uniform particle size distribution [90].

Electrospinning is also recognized as a versatile, simple, and low-cost technique for preparing inorganic nanofibers with a wide range of compositions, uniform diameters, and substantial lengths [91, 92]. Some papers report about electrospun ZnO nanofibers obtained from ZnO precursor solutions mixed with poly(vinylacetate) (PVAc) [93], poly(vinylpyrrolidone) (PVP) [94], or poly(vinyl alcohol) (PVA) [95].

Among vapor-phase techniques, Chemical Vapor Deposition (CVD) is predominantly used for the production of thin films and coatings, particularly in semiconductor manufacturing and materials science, due to its versatility and precision [96]. The CVD technique involves chemical reactions of zinc precursors (in the vapor phase), which give rise to the deposition of a solid material onto a substrate through nucleation and oriented growth. By changing the experimental conditions, such as the distance between substrate and source, gas flow rate, process temperature, and catalyst, it is possible to change the shape, density, and size of ZnO nanostructures [97]. Compared to other vapor processes, CVD is a low-cost, low-maintenance, and effective process for depositing uniform films exhibiting good adhesion to the growing substrate. Besides, the easiness of controlling the growth rate accounts for the high reproducibility of the obtained nanostructures [97].

Solution-based methods for ZnO synthesis offer numerous advantages over vapor-phase methods, including lower costs, milder experimental conditions, better scalability, easier control over particle morphology, and environmental friendliness. They are more versatile and simpler to implement, making them highly attractive for many applications, particularly when working with temperature-sensitive substrates or when large-scale production is desired. However, the choice of method ultimately depends on the specific application requirements, as vapor-phase methods might be preferred for applications requiring high-purity ZnO films or precise thin-film deposition [98].

4 Energy harvesting: the role of ZnO

Energy harvesting involves capturing and converting energy from the environment into usable electrical energy. This energy can originate from various sources, including solar radiation, thermal gradients, kinetic or vibrational energy, and electromagnetic waves [19, 99, 100]. The main objective of energy harvesting is to power small electronic devices, sensors, or systems without relying on external batteries or power supplies, thereby promoting sustainability and minimizing energy waste. Energy harvesting is essential for the development of self-sustaining devices within the Internet of Things (IoT) and for decreasing reliance on batteries, thus fostering the advancement of greener and more efficient technologies [101–103]. Mechanical energy is the most abundant ambient energy source and can be efficiently captured and converted into useful electrical power [104]. Piezoelectric energy harvesting is a highly convenient method for capturing ambient mechanical energy and converting it into electrical power. This is because it operates only through the material intrinsic polarization, without the need for material contact, external voltage source, or magnetic field, as required by

triboelectric, electrostatic, and electromagnetic energy harvesting methods, respectively [105]. According to Priya's theoretical calculation [106], piezoelectric energy harvesting devices have an energy density that is 3 to 5 times greater than that of electrostatic and electromagnetic devices.

Piezoelectric energy harvesting devices have a broad spectrum of applications in various fields, including water applications, transportation, structures, aerial uses, smart systems, microfluidics, wearable and implantable electronics, biomedical devices, and tissue regeneration [19, 107, 108].

As far as ZnO is concerned, several bending beam structures have been built and their piezoelectric properties analyzed for wireless sensor networks [109–111] and portable electronics [112–114]. ZnO nanogenerators are increasingly used in smart cities [115], agriculture [116, 117], or industrial settings to monitor such conditions as temperature, pressure, or structural health without the need for external power sources. ZnO-based energy harvesters can be used as power sensors embedded in buildings, bridges, and roads to monitor their structural integrity [118, 119]. The sensors are self-powered by harvesting mechanical energy from ambient vibrations or environmental factors like wind or traffic. ZnO nanostructures can be integrated into textiles or other flexible materials to create flexible, wearable energy harvesting systems suitable for applications in smart clothing or wearable electronics [113, 120–125]. An example of wearable electronics inserted in shoes is reported in Fig. 6 [126].

The generation of electricity from body movements makes ZnO devices ideal for powering small devices to detect human motions and subtle physiological activities, with potential for motion capture, tactile perception, health monitoring, clinical diagnosis [115], and also for monitoring vital signs, such as heart rate or muscle activity [127–131] (Fig. 7).

5 Recent energy harvesting applications of "bulk" piezoceramic ZnO systems

ZnO piezoceramics have been employed quite extensively to design highly efficient "bulk" (i.e., not incorporated into a polymer matrix) piezoelectric devices. The present paragraph will summarize some recent scientific outcomes.

Kim and co-workers [132] tried to solve the issue related to the design of piezoceramic haptic devices, which usually exhibit high piezoelectric coefficients but show some limits as far as their elastic strain (i.e., the displacement over the entire thickness of the



Fig. 6 Prototype of a piezoelectric film inserted in a shoe. Reprinted with permission from [126]. Copyright Elsevier, 2006

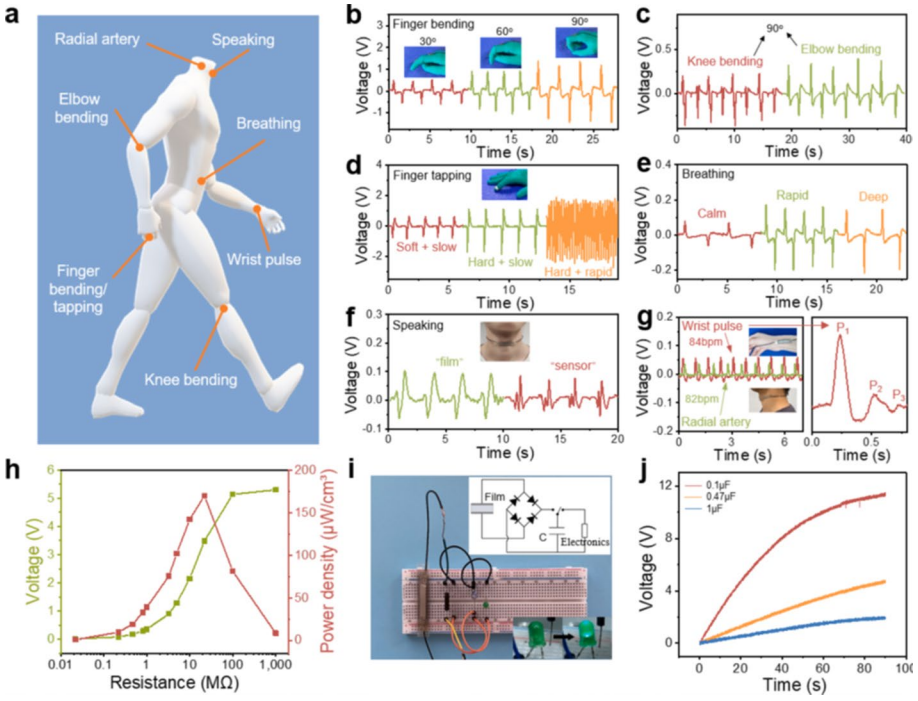


Fig. 7 Example of potential applications of flexible PVDF/ZnO piezoelectric film device converting human motions (**a**), including finger bending (**b**), knee and elbow bending (**c**), finger tapping (**d**), breathing (**e**), speaking (**f**), and radial carotid and wrist pulse (**g**). Power density and instantaneous peak voltage (**h**) of the device as a function of the load resistance at 10 Hz and under repeated pressure of 53 kPa. Circuit diagram for capacitor charging and discharging to lighten a LED lamp. The effective working area is 0.4×1.2 cm.^{2} (i). Representative charging curves of various capacitors (j). Reprinted with permission from [121].
Copyright Elsevier, 2023

material) is concerned. To this aim, a truss-like 3D ZnO hollow nanostructure was manufactured employing proximity field nanopatterning and atomic layer deposition on an SU-8 epoxy layer template (Fig. 8) at four different processing temperatures (namely, 90, 165, 250, and 300 °C). Dual AC resonance tracking piezoresponse force microscopy tests highlighted a piezoelectric coefficient as high as 9.2 pm/V.

Further, around 10% elastic limit was measured through compression tests carried out on the 3D ZnO hollow nanostructure, suggesting its suitability for the design of efficient haptic devices.

Abu Ali et al. [133] exploited plasma-enhanced atomic layer deposition for fabricating ZnO thin films (thickness below 70 nm) deposited either on a poly(ethylene terephthalate) or glass substrate. The deposition on the former substrate accounted for higher values of piezoelectric current and charge (beyond 1.8 nA and 80 pC, respectively) compared to the nanofilms deposited on glass (0.3 nA of piezoelectric current and 30 pC of charge). This finding was ascribed to the high flexibility of the polymer substrate compared to glass. Besides, the increase in deposition temperature accounted for a strengthening of the produced piezoelectric current signal (when mechanical stress was applied along the polar axis in the hexagonal ZnO structure), due to the growth of the deposited film along the (002) crystallographic orientation.

Scanning spreading resistance microscopy was specifically exploited by Synhaivskyi and co-workers [134] to assess the piezoelectric effectiveness of ZnO nanowires (Fig. 9)

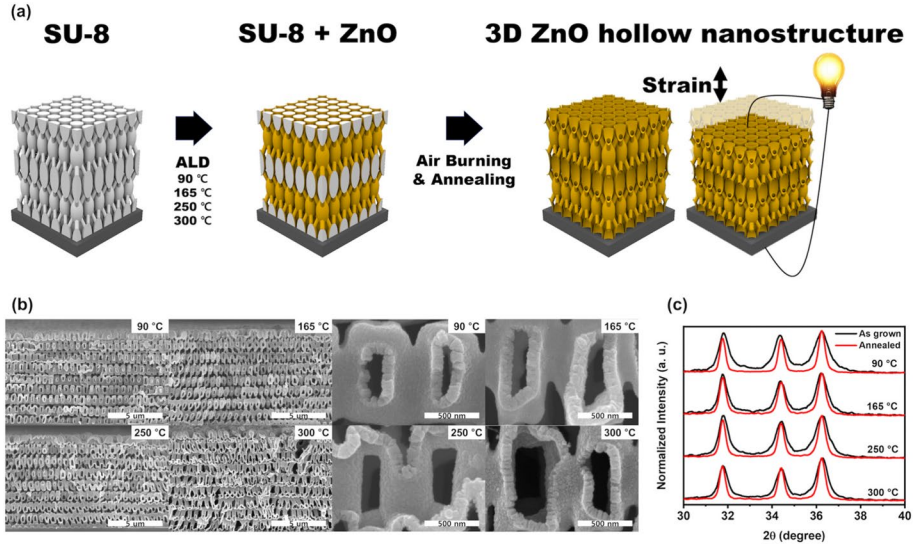


Fig. 8 Conceptual schematics (**a**) and SEM images (**b**) of 3D ZnO hollow nanostructure deposited at 90, 165, 250, and 300 °C after removal of the epoxy template. XRD patterns of 3D ZnO hollow nanostructure before (black) and after additional annealing (red) for each deposition temperature (**c**). Legend: ALD = atomic layer deposition. Reprinted with permission from [132].
Copyright Elsevier, 2020

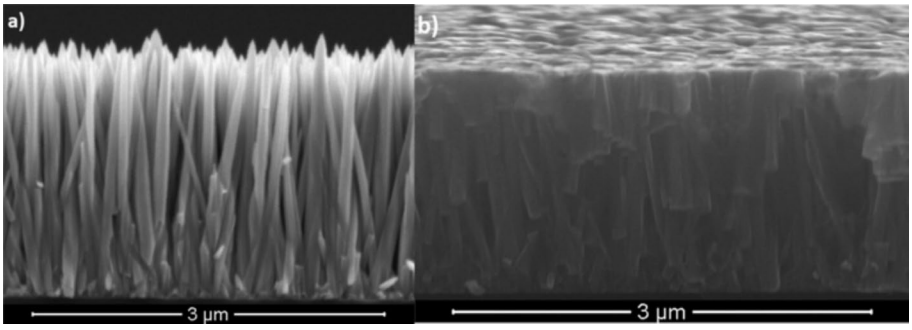


Fig. 9 Cross-sectional (90°) field emission scanning electron microscopy (FESEM) image (**a**) of 2.5% Ga-doped nanowires after CBD deposition. Tilted cross-sectional (84°) FESEM image (**b**) of 2.5% Ga-doped nanowires after encapsulation in a silica matrix and chemo-mechanical polishing (average roughness: 3.2 nm). Reprinted with permission from [134].
Copyright ACS, 2021

doped with either Ga or Al and grown on silicon substrates through chemical bath deposition.

The doping process accounted for a remarkable increase in the electrical conductivity of ZnO nanowires, achieving concentrations of free charge carriers as high as $(7.6 \pm 3.6) \times 10^{19}$ cm^{-3} for the material doped with Ga.

Besides, the ZnO nanowires, even highly doped, showed piezoelectric properties: this finding was ascribed to an augmented surface trap density effect that promoted a Fermi level pinning at the pH values used during the doping processes.

Liu et al. [135] fabricated an interesting piezotronic structure made of ZnO nanoplatelets, which combines the piezoelectric effect with semiconducting features, suitable for the design of smart micro/nano-electromechanical systems, nanorobotics, and human–machine interfacing devices. In particular, a preferred orientation of inner ZnO nanoplatelets accounted for better carrier transport control, thus increasing the electrical

conductivity of the bulk material, working at 200–400 MPa pressure. In these conditions, the measured maximum sensitivity and related gauge factor were as high as 1.149 $\mu S\ m^{-1}\ MPa^{-1}$ and 467–589, respectively.

Polewczyk et al. [136] exploited x-ray diffraction and atomic force microscopy techniques to investigate the role of thermal treatments and sputtering gas composition on the piezoelectric response of ZnO thin films (thickness: 300 nm) in heterostructure-based devices. More specifically, the use of a variable deposition temperature between room temperature and 573 K, together with the introduction of 75% oxygen in the sputtering gas, accounted for the obtainment of ZnO films on a silica/silicon substrate with very low surface roughness (about 2–3 nm), good orientation along the c-axis and columnar grains (with a diameter of about 45 nm in the surface plane). Further, the growth of these structures on bottom titanium electrodes induced a moderate piezoelectric response, with 1.9 ÷ 0.3 pm/V for the depositions performed at 573 K.

Large (i.e., with a surface area larger than 30 cm^2) single ZnO crystals (possibly doped with Ga) were prepared through a hydrothermal process as piezocatalytic materials by Wang and co-workers [137], who investigated the catalytic hydrogen evolution from pure water. When this latter was excited by ultrasound in the dark, a significant hydrogen production activity was observed, with a maximum rate beyond 5900 μmol/h m^2. Besides, both the distribution and magnitude of the piezoelectric potential of the synthesized ZnO single crystals were found to be strictly dependent on thickness and exposed crystal plane.

Nikolaev and co-workers [138] demonstrated the possibility of remarkably enhancing the efficiency of the piezoelectric chemosensors by employing ZnO nanorod arrays synthesized on metal contacts as sensing elements. To this aim, different synthetic strategies (namely, hydrothermal, electrochemical, and carbothermal techniques) were successfully employed. In particular, the carbothermal process accounted for the obtainment of perfect, dense, and homogeneous nanorod arrays with good piezoelectric properties (Fig. 10), suggesting their suitability for the design of efficient bulk resonators with noticeable photo and gas sensitivity.

Golovanov et al. [139] succeeded in synthesizing thick piezoelectric ZnO films fabricated on both sides of various substrates (namely, lithium niobate and quartz plates, and Kapton films) using the magnetron sputtering technique. To fix the issue related to the different thermal expansion coefficients of the ZnO films and the substrates, the sputtering conditions were optimized: this way, it was possible to obtain ZnO films

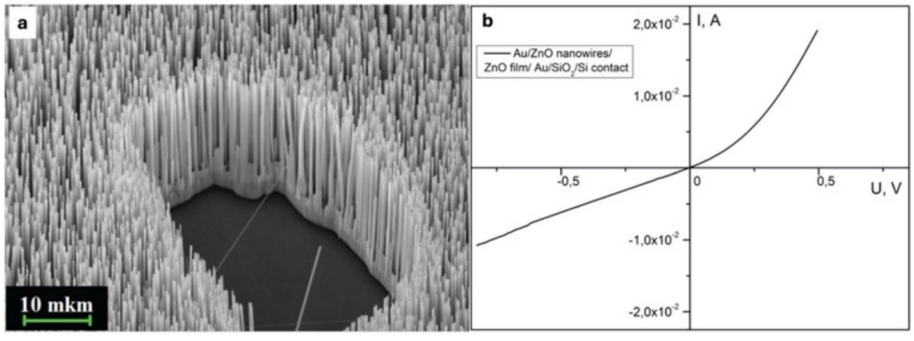


Fig. 10 SEM image (**a**) of nanorods obtained by carbothermal synthesis on the Au electrode. The current–voltage characteristic (**b**) of the Au/ZnO nanorods/ZnO film/Au/SiO_2/Si structure. Reprinted from [138] under CC-BY 3.0 License

with a thickness of up to 15 μm, grain size of 0.3 μm, high piezoelectric modules (i.e., 7.5 pC/N), providing, after the application of mechanical stress, an electrical voltage of around 35 mV, enough to design effective autonomic micro-energetic energy-store systems.

Tran and co-workers [140] exploited density functional theory calculations to demonstrate the possibility of restoring the buckling of ultrathin 2D ZnO sheets, and, therefore, their piezoelectric features, through the incorporation of defects (i.e., adsorbed O, or O/Zn vacancies) into the piezoceramic material. In particular, the presence of 25% Zn vacancy concentration in a 1.48 nm thick ZnO sheet resulted in an e_{33} value that exceeded the bulk by 120%. These results suggested the suitability of the surface-modified ZnO nanosheets for the design of piezoelectric nanogenerators for energy harvesting and efficient nano-based optoelectronic devices.

Similarly, a recent study from Yu et al. [141] utilized (0001)-oriented ZnO single crystals (thickness of about 0.2 mm) for the fabrication of Bulk Acoustic Wave resonators, i.e., radio frequency devices able to convert X-ray dose rate into a resonant frequency offset (Fig. 11). The resonant frequency offset of the detector was recorded under dark field and X-ray irradiation through the readout circuit, made of a frequency mixing circuit, an oscillator circuit based on a Pierce oscillator circuit structure, and an STM32 microcontroller. Changes in X-ray dose rate were observed based on the variation of the resonant frequency, which, in turn, was affected by the changes in the ZnO piezoelectric field as a consequence of the X-ray irradiation.

To summarize, Table 3 collects the main research outcomes for the systems discussed in the present paragraph.

6 Recent energy harvesting applications of polymer-ZnO piezoelectric systems

For energy harvesting applications, ZnO fillers can also be embedded into inert polymers primarily to combine the advantages of both materials. In fact, ZnO, as a ceramic material, is often brittle and rigid on its own. By incorporating the filler into a polymer matrix, the resulting composite becomes more flexible and mechanically robust, allowing the device to withstand repeated deformations without cracking [142]. The polymer matrix helps distribute mechanical stress evenly across the composite, protecting the piezoelectric filler from damage and increasing the device's endurance [143, 144]. Also, by varying the amount of piezoelectric filler and the type of polymer, the mechanical and electrical properties of the composite can be finely tuned for specific applications [145].

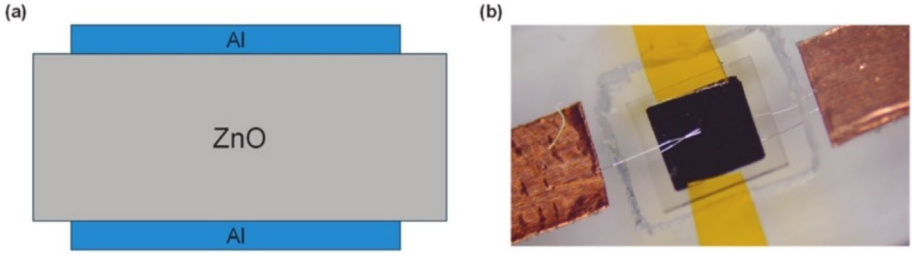


Fig. 11 Schematic diagram (**a**) and photo (**b**) of the ZnO single crystal Bulk Acoustic Wave detector. ZnO single crystal has a size of $5 \times 5 \times 0.2$ mm.^{3} and the electrodes of Al have a thickness of 100 nm. Reprinted with permission from [141].
Copyright Elsevier, 2024

Table 3 Main research outcomes for "bulk" piezoceramic ZnO systems

Authors	System	Main outcomes	Ref
H. Kim et al	3D ZnO hollow nanostructure	9.2 pm/V piezoelectric coefficient	[132]
T. Abu Ali et al	ZnO thin films deposited on PET substrate	high piezoelectric current and charge values (beyond 1.8 nA and 80 pC, respectively)	[133]
O. Synhaivskyi et al	ZnO nanowires doped with Ga or Al	High concentrations of free charge carriers (7.6×10^{19} cm^{-3}) when ZnO are doped with Ga	[134]
S. Liu et al	ZnO nanoplatelets	Under 200–400 MPa pressure, high maximum sensitivity and related gauge factor of 1.149 μS m^{-1} MPa^{-1} and 467–589, respectively	[135]
V. Polewczyk et al	ZnO thin films deposited on Ti electrodes	Moderate piezoelectric response ($1.9 \div 0.3$ pm/V) for the depositions performed at 573 K	[136]
B. Wang et al	Single ZnO crystals	Distribution and magnitude of the piezoelectric potential strictly dependent on crystal thickness and exposed crystal plane	[137]
E. Golovanov et al	ZnO nanorod arrays	High piezoelectric modules (7.5 pC/N) and electrical voltages of ca. 35 mV	[139]
K. Tran et al	Ultrathin 2D surface-modified ZnO sheets	25% Zn vacancy concentration accounted for e_{33} values exceeding the bulk by 120% (sheet thickness of 1.48 nm)	[140]
Z. Yu et al	Single ZnO crystals	Suitability for the design of Bulk Acoustic Wave Resonators	[141]

The presence of the polymer, which acts as an insulator, prevents leakage of electrical charge and helps to accumulate the charge generated by the piezoelectric filler [146]. Also, it allows for a larger surface area to be subjected to mechanical stress, which can increase the amount of energy harvested [147]. From the fabrication point of view, polymers are generally cheaper and easier to process than ceramics or single-crystal piezoelectric materials [143, 145, 148]. This allows for the development of devices that can be integrated into clothing, wearables, and soft robotics, fabricated into various shapes and sizes, and versatile for a wide range of energy harvesting applications, from small-scale sensors to large-scale structural health monitoring systems [149]. The most employed matrices for the preparation of piezoelectric composites are poly(dimethylsiloxane) (PDMS) [52, 150, 151] and photocurable resins [152, 153]. PDMS is a polymer characterized by such important properties as flexibility, chemical stability, biocompatibility, hydrophobicity, and high thermal and thermo-oxidative stability [154]. It is widely used in the fabrication of flexible devices because of its mechanical properties [155]. Cauda et al. [52] used PDMS to prepare composites containing ZnO particles with different morphologies (i.e., microwires, multipods, and desert roses) and aspect ratios, synthesized by a hydrothermal process, intending to investigate the piezoelectric output power dependence on the filler morphologies used. They found that an output voltage of about 9 V and a maximum power of 55 mW were obtained when 40 wt.% of the highest aspect-ratio ZnO filler (i.e., the microwires) was used (Fig. 12).

Jeronimo et al. [150] prepared PDMS/ZnO nanocomposites using two different ZnO morphologies (i.e., nanoflowers and nanospheres) at different loadings (up to 10 wt.%). The composites containing nanoflowers produced a higher and more stable electrical response compared to the commercial nanoparticles, hence demonstrating that the proper selection of the geometry of the nanofillers is of paramount importance to maximize the piezoelectric response.

Zhang et al. [151] sought to enhance the dielectric and piezoelectric properties of PDMS by incorporating spherical ZnO microparticles at four different volume fractions (namely, 14, 24, 34, and 44 v.%). The ZnO microparticles were aligned via dielectrophoresis, improving the connectivity between ZnO interfaces, and thereby boosting

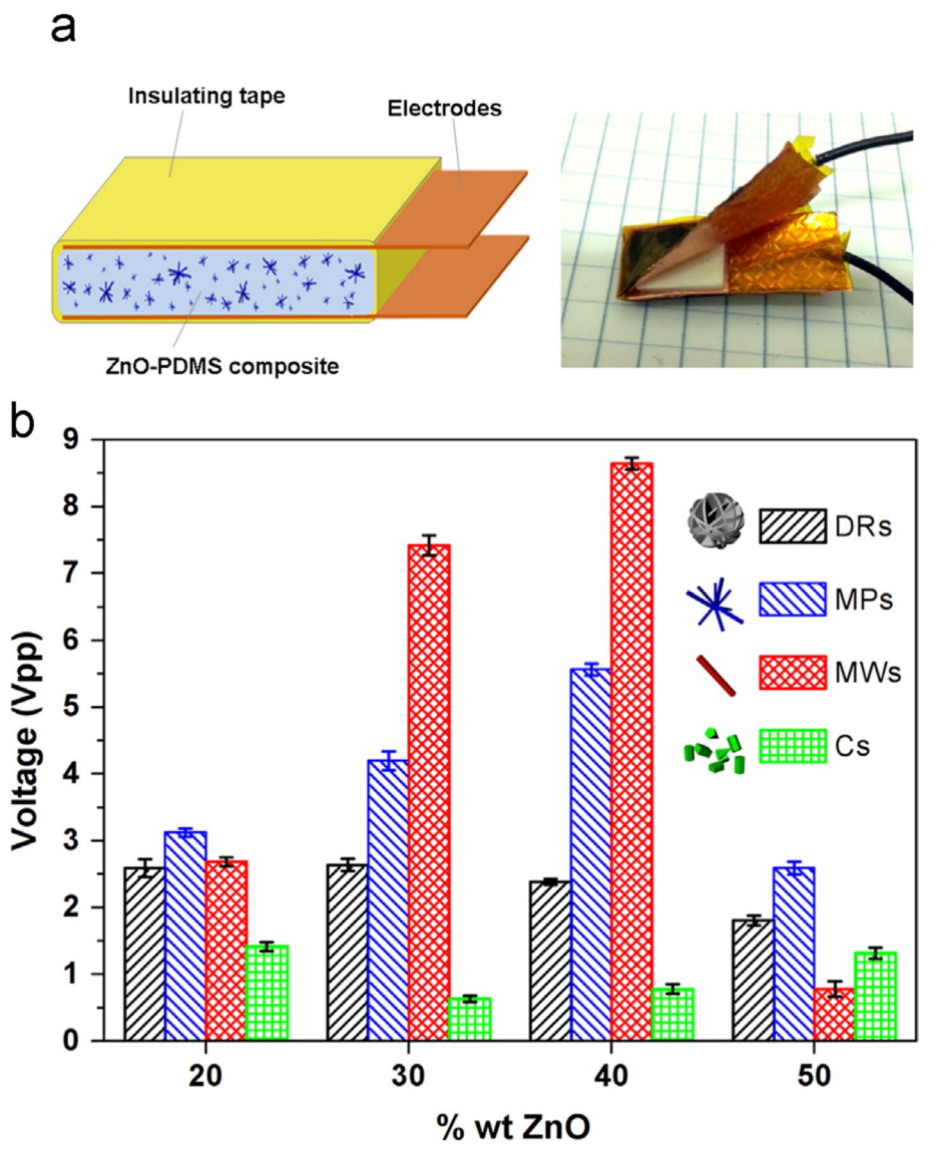


Fig. 12 Schematic representation and photo of the PDMS/ZnO device assembled within the electrodes. PDMS/ZnO has dimensions of 10×10×1 mm^3; PMMA and the copper-metalized rectangles are 20×10 $mm.^2$ (**a**); peak-to-peak output voltages (**b**) obtained after compression (at 75 Hz of oscillating frequency and 0.2 mm peak-to-peak displacement) of the PDMS/ZnO composites based on the four different ZnO morphologies at different ZnO filler concentrations (i.e., 20, 30, 40, and 50 wt.%). Legend: DRs = desert roses, MPs = multipods, MWs = microwires, Cs = commercial particles. Reprinted with permission from [52].
Copyright Elsevier, 2015

the overall piezoelectric performance. Notably, at a low volume fraction of 14 v.%, the d_{33} value of the oriented sample exhibited a significant increase compared to the unoriented one (0.4 vs. 0.05 pC/N, respectively). Beyond 24 v.% of ZnO, the d_{33} of the oriented sample showed only a small increase, reaching a saturation point. This behavior contrasted with randomly oriented ZnO composites, where d_{33} improved significantly at higher filler loadings. When the volume fraction was 44%, the oriented composite demonstrated nearly doubled d_{33} compared to the unoriented composite (0.52 pC/N vs. 0.27 pC/N, respectively).

UV-curable systems are widely employed in the preparation of piezoelectric systems due to several key advantages, meeting the complex demands of piezoelectric device

fabrication while offering efficiency and versatility [55]. UV curing is compatible with advanced fabrication techniques like photolithography. This enables high-resolution patterning, which is essential for creating intricate structures in microelectromechanical systems (MEMS) and other miniaturized piezoelectric devices [152, 155–157].

Prashanthi et al. [152] incorporated 20 wt.% of ZnO nanoparticles into SU-8 photoresist. More specifically, a layer of SU-8 was spin-coated onto a silicon substrate featuring a Ti/Au deposition and subsequently underwent thermal treatment to remove the residual solvent. Notably, the film exhibited a d_{33} coefficient of 6.2 pm/V, aligning closely with the values reported for bulk ZnO.

Kandpal et al. [156] found that the resonant frequency response of the piezoelectric device based on Su-8/ZnO, increased from 15 to 23 pm/V with increasing the ZnO loading from 5 to 20 wt.%. In another work, SU-8/ZnO at 15 wt.% of ZnO exhibited open circuit voltages of 570 mV, when stressed by regular finger pressing [157].

Malucelli and co-workers employed bis-phenol A ethoxylate diacrylate (Ebecryl 150) for preparing UV-cured composite films filled with ZnO micro- and nano-objects [56, 158, 159]. In particular, the influence of the different ZnO morphologies (incorporated at 4 wt.% loading) on the piezoelectric response of 150 μm thick films was studied [56]. Flower-like morphologies showed the best piezoelectric performance at both 150 Hz and at the resonance frequency, reaching a maximum RMS voltage of 0.914 mV when 5.79 g of acceleration was applied. These findings were attributed to the fact that, in the flower-like morphologies, a higher amount of the (002) crystallographic planes could be found parallel to the applied mechanical solicitation and, thus, more effective from a piezoelectric point of view.

In a further research effort, the same group assessed the impact of the ZnO loading (ranging from 4 to 20 wt.%) on the piezoelectric performance of the UV-cured films [158]: RMS output voltages of 4.94 mV and 1.85 mV at 5 g of acceleration were measured for the composite films embedding 20 wt.% flower-like and needle-like ZnO, respectively.

To enhance the piezoelectric responses of these Ebecryl150/ZnO composites, Signore et al. added cellulose nanocrystals (CNCs), a powder vapor-deposited AlN layer onto the top surface, and an anchored proof mass on the beam tip [159]. They demonstrated that CNCs negatively impacted the piezoelectric properties of the composite films compared to those with ZnO. This finding was attributed to the lower crystallinity of cellulose nanocrystals and their poorer interfacial adhesion with the polymer matrix. On the other hand, the deposition of a nitride layer on the flower-like ZnO composite film accounted for a significant increase in the RMS voltage from 1.0 to 3.9 mV. This output voltage further improved with the addition of a proof mass, reaching 4.5 mV.

ZnO was also added to ferroelectric polymers such as poly(vinylidene fluoride) (PVDF) [160–164] and poly(vinylidene fluoride-*co*-trifluoroethylene) copolymer (PVDF-TrFE) [144] for improving the piezoelectric performances of the polymer device.

PVDF is the most studied polymer as a nanogenerator, due to its biocompatibility, flexibility, and good piezoelectric features. The β-phase of PVDF is polar and shows the strongest ferroelectric and piezoelectric response [165]. ZnO nanoparticles can enhance the β-phase formation and the piezoelectricity of PVDF polymer. Considering that ZnO is inherently piezoelectric due to its non-centrosymmetric wurtzite crystal structure, it does not require poling [166]. However, poling is often necessary when

incorporating a piezoelectric material into a polymer matrix to form a composite with an overall enhanced piezoelectric response. This is mainly because the polymer component (e.g., PVDF) contains randomly oriented dipoles that require alignment using an external electric field. Poling facilitates the alignment of these dipoles and may also improve interfacial charge transfer between ZnO and the polymer, thereby enhancing the composite's performance [167, 168]. The process permanently polarizes the material, so careful control and optimization are crucial to ensuring the reliability and efficiency of piezoelectric devices [55, 166].

Among the most recent works on PVDF composites, Mahapatra et al. grew ZnO nanorods by hydrothermal method and incorporated them into a PVDF matrix in the concentration range of 5–15 wt.% [143]. The open-circuit voltage of these systems increased from approximately 4 to 14.6 V as the ZnO nanorod loading in the polymer matrix increased from 0 to 10 wt.%; besides, further increase in ZnO nanorod loading provided a detrimental effect on the piezoelectric behavior (Fig. 13).

The observed piezoelectric trend (below 10 wt.% ZnO nanorod loading) was attributed to the presence of the PVDF β-phase, while the subsequent decreased output voltage was ascribed to changes in the dielectric constant and remnant polarization. The system embedding 10 wt.% ZnO was employed for developing a shoe insole pedometer, which was successfully tested over 5000 steps at various walking frequencies, ranging from 0.5 to 2 Hz, and speeds between approximately 1.4 and 5.5 km/h.

Pursuing this research, the same group designed a self-powered UV sensor with high responsivity by combining a flexible ZnO (in the form of nanorods)-PVDF piezoelectric nanogenerator and a photodetector for continuous real-time monitoring of UV radiation [169]. The device showed remarkable performance, as witnessed by 93% sensitivity, 7.14 V responsivity, 0.67 s response time, and 4 s recovery time.

Li et al. [144] modified ZnO nanoparticles through the concurrent addition of a dispersant (n-propylamine) and a silane coupling agent (i.e., perfluorooctyltriethylsilane) and were then incorporated into PVDF-TrFE (Fig. 14). The average d_{33} value of the film containing modified ZnO was around 34.7 pC/N, which was remarkably higher than that of the unfilled PVDF-TrFE film (about 20.0 pC/N). The average value of the output

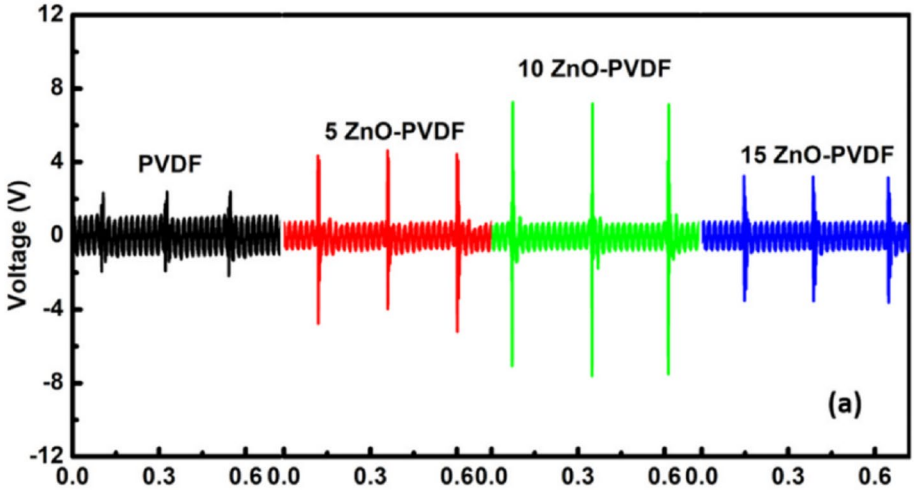


Fig. 13 The open circuit voltage PVDF/ZnO-based device with different ZnO concentrations. Reprinted with permission from [143].
Copyright Elsevier, 2023

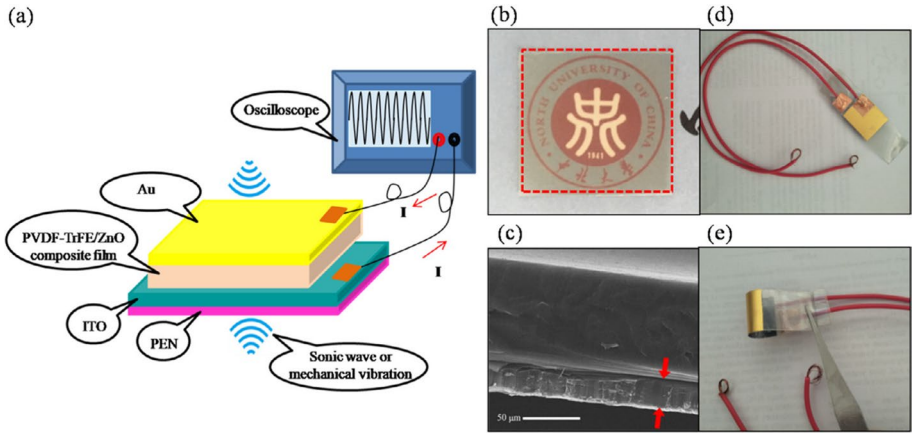


Fig. 14 The schematic structure of the device. The thickness of the whole film was determined from the SEM image of the cross-section and was approximately 22 μm (**a**). Image showing the optical transmittance of the PVDF-TrFE/ZnO composite film after ZnO modification with silane (**b**). Side-view SEM image of the device (**c**). Digital image of the device (**d**) and its flexibility (**e**). Legend: ITO = Indium Tin Oxide; PEN = poly(ethylene naphtalate); PVDF-TrFE = poly(vinylidene fluoride-*co*-trifluoroethylene) copolymer. Reprinted with permission from [144]. Copyright Elsevier, 2019

voltage of the fabricated piezoelectric nanogenerator obtained by sandwiching the film between ITO and Au layers was 2.65 V (the unfilled film exhibited an output voltage of 2.13 V). After 1000 testing cycles, the output voltage of the device remained stable at 2.40 V, demonstrating the generator's excellent mechanical durability and its potential suitability for flexible, smart device applications.

Poly(acrylonitrile) (PAN) [170] gained attention as a ferroelectric polymer because it may exhibit a better piezoelectric response than PVDF, despite a limited capacity to convert mechanical energy into electrical energy [171]. PAN/ZnO composites were prepared by solution casting after mixing PAN and two different types of ZnO at 5 wt.% loading, namely: spherical ZnO (ZnP) obtained by precipitation and ZnO nanowires (ZnW) synthesized through a hydrothermal method. It was found that, without any external poling, all the films showed increasing output voltage with increasing tapping frequency. More specifically, for the PAN film, the voltage rose from approximately 1 to 14.3 V; for PAN/ZnP, it increased from 10 to 40 V, and for PAN/ZnW, from 16 to 52 V as the frequency was raised from 1 Hz to 3.1 Hz, respectively.

Zhu et al. [172] exploited electrospinning to obtain PVDF membranes incorporating cellulose nanofibers loaded with ZnO (through the hydrothermal method). The resulting composite membranes showed longitudinal piezoelectric coefficients (d_{33}) of 31 ± 2.07 pC/N; besides, the application of a 45 N force accounted for open-circuit voltage and short-circuit current of 11.8 V and 452 nA, respectively.

Motora and co-workers developed a piezoelectric nanogenerator comprising a ZnO/PVDF membrane obtained through electrospinning [173]. Under 12 N force, this nanogenerator could harvest power density, voltage, and output current of 20.1 mW/m^2, 50 V, and 1.15 μA, respectively. Besides, the energy scavenging provided by the nanogenerator was enough to light 20 green LEDs and display an LCD timer for 1 s. Finally, the device showed outstanding cyclic charging and discharging properties, making it potentially suitable for practical energy harvesting applications.

Rahsepar et al. employed the Taguchi design experiment for optimizing the figure of merit of KNN-0.8ZnO embedding polyvinylidene fluoride-hexafluoropropylene

copolymer at different loadings (namely 20, 30, and 40 wt.%), and prepared by cold sintering (at 400 MPa, 200 °C for two hours) [174]. 20 wt.% of the copolymer accounted for a d_{33} coefficient of 43.2 pC/N, showing the best figure of merit (i.e., 1.95 pm^2/N).

Moezzi and co-workers incorporated different amounts of ZnO nanoparticles (from 5 to 40 wt.%) into a poly(lactic acid) matrix, aiming to obtain low-cost piezoelectric "sustainable" films [175]. Applying 1 kgf impact pulse pressure and working at 3 Hz frequency accounted for high piezoelectric features, as evidenced by short-circuit current values and normalized peak-to-peak open circuit voltages as high as 167.1 nApp/g, and 8.55 Vpp/g, respectively.

Huang et al. designed novel polyacrylonitrile nanofiber-based flexible piezoelectric sensors embedding MXene and polydopamine-modified ZnO (3 to 10 wt.% ZnO loading) [176]. The devices showed outstanding linearity and high sensitivity, up to about 29 V/N. Besides, they highlighted fast swift response and recovery times (respectively of 49 and 40 ms), together with excellent mechanical behavior and durability.

Wang et al. exploited a one-pot synthesis method for obtaining piezoelectric hydrogels: to this aim, ZnO nanoparticles (up to 4.4 wt.% loading) and carboxylated multiwalled carbon nanotubes (at 22.2 wt.% loading) were incorporated into a hydrogel made of poly(vinyl alcohol), agar, and tannic acid [177]. The piezoelectric hydrogel with the highest zinc oxide loading was able to produce stable piezoelectric signals (93.4 mV voltage generated under the impact of a 100 g weight, 50 mm free fall), suitable for energy harvesting purposes.

Misra and co-workers synthesized solid and hollow zinc oxide nanorods, to be employed with PDMS in the manufacturing of piezoelectric touch and bending sensors [178]. In particular, under the application of 400 nN force, the piezoelectric potential values of hollow and solid zinc oxide nanorods-based sensors were about 1200 and 200 mV, respectively. These findings were ascribed to the different aspect ratios of the two nanostructures.

Taleb et al. exploited two different techniques, namely spray coating and casting, for preparing ZnO/poly(vinylidene fluoride-trifluoroethylene) copolymer composite films [179]. The use of the casting method and the incorporation of 20 wt.% of zinc oxide ensured a good piezoelectric response, with a d_{33} of 48.93 pm/V and a high sensitivity (about 18.5 mV/N): these characteristics suggested the potential of the obtained films both as tactile sensors in a gripping robot and as wearable devices, able to monitor the movement in human arms.

Wang and co-workers investigated the piezoelectric features of electrospun poly(vinylidene fluoride-trifluoroethylene) copolymer nanofibers loaded with AlN (at 0.1 wt.%) and ZnO (at different loadings, namely, 0.5, 1, and 1.5 wt.%) [180]. In particular, the presence of 1.5 wt.% of zinc oxide allowed for measuring 23 V open-circuit voltage and 65 nA short-circuit current in the final device, hence demonstrating its suitability for efficiently monitoring human movements through the recognition of signal features from several finger postures.

He et al. designed and developed a self-powered piezoelectric sensor made of 3D porous fluorine-containing polyimide and ZnO nanoparticles (5–20 wt.% loading), exploiting a water vapor-induced fast phase separation technique [181]. 15 wt.% of zinc oxide accounted for exceptional piezoelectric sensitivity (0.75 V/N), high voltage output

(4 V), fast response and recovery time (15 and 20 ms, respectively), and remarkable durability (beyond 9000 cycles).

Fernandez-Gil and co-workers demonstrated that aligning ZnO microrods (at 5–30 wt.% loading) in 3D-printed polycaprolactone in the presence of conductive particles like thermally reduced graphene oxide (at 0.2 or 0.5 wt.%) allows for obtaining high-performing piezoelectric devices with boosted piezo-response [182]. More specifically, the composites embedding 30 wt.% of zinc oxide and 0.5 wt.% of thermally reduced graphene oxide showed maximum voltage generation of about 142 and 696 mV, respectively during the application of a remote pressure produced by ultrasonic waves and the application of a direct contact mechanical pressure exerted by a linear actuator.

To summarize, Table 4 collects the main research outcomes for the systems discussed in the present paragraph.

7 Challenges and limitations of ZnO-Based piezoelectric Nano/microstructures and composites

ZnO has been widely studied as piezoelectric material due to its intrinsic non-centrosymmetric wurtzite structure, ease of synthesis, and environmental compatibility [38, 41] Additionally, ZnO–polymer composites have gained traction for their combination of mechanical flexibility and enhanced piezoelectric response [52]. Despite these advantages, both ZnO and its polymer composites face notable challenges that limit their practical applications. A key limitation lies in material quality and defect control. In ZnO nanostructures, such defects as oxygen vacancies and zinc interstitials can lead to charge screening, reducing the piezoelectric output. [183, 184] In composites, poor dispersion or aggregation of piezoelectric filler within the polymer matrix can cause inconsistent performance and low efficiency [158, 185]. Mechanical stability is also a concern. In fact, ZnO nanowires are prone to fracture; besides, in composites, the interface between ZnO and the polymer often suffers from weak adhesion, limiting stress transfer and device durability [186]. Although ZnO itself does not require poling, poling becomes essential in ZnO-polymer composites to align the polymer dipoles and optimize the piezoelectric performance. This step must be carefully controlled to avoid poor reproducibility and low output [167, 168]. In terms of output performance, both systems generally produce low voltages and currents, with energy conversion efficiencies affected by parasitic losses, charge trapping, and non-optimized interfaces. Therefore, further research efforts are required to solve these issues in the coming years.

Scalability and integration represent major bottlenecks. Achieving uniform ZnO nanostructure orientation or consistent ZnO dispersion in polymers over large areas is challenging. Moreover, many fabrication methods lack compatibility with standard manufacturing processing [187]. Finally, environmental stability and biocompatibility present concerns. ZnO can degrade when exposed to moisture [188] or UV light radiation [189–191]. While ZnO composites offer some protection, their long-term performance requires further validation [192]. In summary, although ZnO-based piezoelectric structures and their composites show great potential, it is crucial to address issues related to material defects, mechanical integrity, output efficiency, interfacial engineering, and process scalability for them to transition into reliable, real-world devices.

Table 4 Main research outcomes for polymer-ZnO piezoelectric systems

Authors	System	Main outcomes	Ref
V. Cauda et al	ZnO particles with different morphologies in PDMS	ZnO microwires at 40 wt.% accounted for an output voltage of about 9 V and a maximum power of 55 mW	[52]
K. Jeronimo et al	ZnO nanoflowers in PDMS	More stable electrical responses compared to devices embedding the commercial nanoparticles	[150]
X. Zhang et al	Spherical ZnO microparticles in PDMS	d_{33} values of 0.4 and 0.52 pC/N respectively with 14 and 44 v.% of ZnO loadings	[151]
K. Prashanthi et al	ZnO nanoparticles in SU-8	ZnO nanoparticles at 20 wt.% accounted for d_{33} values of 6.2 pm/V	[156]
M. Kandpal et al	ZnO particles in SU-8	ZnO nanoparticles at 20 wt.% accounted for d_{33} values of 23 pm/V	[142]
B. Krishna et al	ZnO particles in SU-8	ZnO nanoparticles at 15 wt.% accounted for open circuit voltages of 570 mV	[157]
G. Malucelli et al	ZnO flowers in a UV-curable acrylic resin	At 4 wt.% loading, a maximum RMS voltage of 0.914 V was achieved under 5.79 g of acceleration	[56]
D. Duraccio et al	ZnO flowers or needles in a UV-curable acrylic resin	At 20 wt.% loading, a maximum RMS voltage of 4.94 and 1.85 mV was achieved under 5 g of acceleration for the composites embedding flowers or needles, respectively	[158]
M.A. Signore et al	ZnO flowers and CNCs in a UV-curable acrylic resin	3.9 mV RMS voltage was achieved when a AlN layer was deposited on the composite films	[159]
A. Mahapatra et al	ZnO nanorods in PVDF	10 wt.% of ZnO accounted for 14.6 V of open-circuit voltage	[143]
A. Mahapatra et al	ZnO nanorods in PVDF	High piezoelectric performance (93% sensitivity, 7.14 V responsivity, 0.67 s response time, and 4 s recovery time)	[169]
J. Li et al	Silane coupling agent-modified ZnO particles in PVDF-TrFE	Average d_{33} value of 34.7 pC/N and output voltage of 2.65 V (which decreased to 2.40 V after 1000 testing cycles)	[144]
G. Kaur et al	Spherical ZnO or ZnO nanowires in PAN	At 5 wt.% loading, spherical ZnO and ZnO nanowires accounted for 14.3 and 40 V output voltages (at 1 Hz frequency)	[170]
Q. Zhu et al	Cellulose nanofibers loaded with ZnO in PVDF	d_{33} values of about 31 pC/N, 11.8 V open-circuit voltage and 452 nA short-circuit current (applying 45 N force)	[172]
K. G. Motora et al	ZnO/PVDF electrospun membranes	Under 12 N force, 20.1 mW/m^2, 50 V, and 1.15 μA harvested, respectively	[173]
H. Rahsepar et al	KNN-0.8ZnO embedding PVDF-hexafluoropropylene	At 20 wt.% of copolymer, d_{33} values of 43.2 pC/N	[174]
M. Moezzi et al	ZnO nanoparticles in poly(lactic acid)	At 40 wt.% loading, short-circuit current values and normalized peak-to-peak open circuit voltages as high as 167.1 nApp/g, and 8.55 Vpp/g, respectively	[175]
Y. Huang et al	PAN nanofiber sensors embedding MXene and modified ZnO	Linearity and high sensitivity up to 29 V/ N; fast swift response and recovery times (49 and 40 ms, respectively)	[176]
H. Wang t al	Hydrogels embedding ZnO nanoparticles and carboxylated multi-walled carbon nanotubes	Stable piezoelectric signals (93.4 mV voltage generated under the impact of a 100 g weight, 50 mm free fall)	[177]
M. Misra et al	Hollow and solid ZnO nanorods in PDMS	Under 400 nN force, 1200 and 200 mV piezoelectric potential values of hollow and solid ZnO	[178]
S. Taleb et al	ZnO particles in PVDF-TrFE	At 20 wt.% loading, d_{33} of 48.93 pm/V and a high sensitivity (about 18.5 mV/N)	[179]
J. Wang et al	Electrospun PVDF-TrFE embedding ZnO and AlN	0.1 wt.% of AlN and 1.5 wt.% of ZnO accounted for 23 V open-circuit voltage and 65 nA short-circuit current	[180]
P. He et al	ZnO nanoparticles in 3D porous fluorine-containing polyimide	At 15 wt.% loading, exceptional piezoelectric sensitivity (0.75 V/N), high voltage output (4 V), fast response and recovery time (15 and 20 ms, respectively), and remarkable durability (beyond 9000 cycles)	[181]

Table 4 (continued)

Authors	System	Main outcomes	Ref
F. Fernández-Gil et al	ZnO microrods and reduced graphene oxide in 3D-printed polycaprolactone	30 wt.% of ZnO and 0.5 wt.% of thermally reduced graphene oxide accounted for maximum voltage generation of ~ 142 mV (applying a remote pressure produced by ultrasonic waves) and 696 mV (applying a direct contact mechanical pressure exerted by a linear actuator)	[182]

8 Future perspectives

The advancement of ZnO-based piezoelectric nano/microstructures and composites is expected to be driven by innovative material combinations and intelligent design strategies. Hybridization with other functional materials like ferroelectrics, two-dimensional materials (e.g., MoS_2, graphene), and conductive polymers [22, 193, 194], holds significant promise for enhancing piezoelectric performance, mechanical adaptability, and multifunctionality. In parallel, doping approaches are being actively explored to modulate ZnO's electrical properties, minimize charge screening, and improve piezoelectric efficiency. [38, 42]. Furthermore, integrating artificial intelligence (AI) and machine learning could be a powerful way to speed up material optimization, guide device design, and adjust processing parameters more accurately [195–197]. These strategies, together with ongoing efforts to develop scalable and compatible fabrication techniques, will be pivotal in advancing ZnO-based piezoelectric systems toward practical applications in wearable electronics, self-powered sensors, and next-generation energy harvesting technologies.

9 Conclusions

The piezoelectric properties of ZnO are currently very interesting and are attracting increasing attention not only from academia but also from industry. Although its piezoelectric properties are lower than those of other piezoceramics like $BaTiO_3$ and lead zirconate titanate, ZnO is a lead-free and low-cost material. In addition, it can be easily processed into different shapes and morphologies, each with different piezoelectric properties and a high degree of tunability according to the piezoelectric device to be designed and implemented. It is also worth noting that, unlike perovskite piezoceramics, crystallographically oriented ZnO micro- and nanostructures do not require external poling for their piezoelectric use, notwithstanding the possibility of exploiting doping processes on ZnO, which have already demonstrated their high potential for increasing the overall piezoelectric efficiency.

All these characteristics highlight the potential of ZnO both as a single piezo crystal grown on a specific substrate with an individual shape/morphology and as a piezo filler in various thermoplastic and thermosetting polymer matrices that do not exhibit any piezoelectric property. Besides, it exhibits piezoelectric features even without polarization. When ZnO structures are incorporated into a polymer matrix, they can still generate an electrical response under mechanical deformation even without polarization. The piezoelectric behavior depends on how ZnO is distributed and oriented within the polymer. If ZnO is well-aligned in a certain direction and evenly distributed in the polymer matrix, the piezoelectric response can be more effective, as it allows for better exploiting coherent and additive contributions from each piezoelectric domain. However, aligning the ZnO structure to maximize its piezoelectric response can be somewhat challenging and costly. A not-very-high piezoelectric response can still be useful in various

applications, especially where the main focus is on mechanical flexibility, cost-effectiveness, or specific material properties over strong piezoelectric effects. In particular, in flexible electronics and wearables, materials with a low piezoelectric response might be preferred when mechanical flexibility is prioritized over high piezoelectric sensitivity.

However, some current limitations must be overcome to widen the use of this piezoceramic. First, despite the large number of ZnO micro- and nano-structures, the current research is somewhat limited to the utilization of only a few of them, particularly referring to such nano-objects as nano-rods/needles, nanosheets, and nanobelts. Conversely, the exploration of the piezoelectric characteristics of other ZnO structures (like flowers, helixes, whiskers, hierarchical (nano)rods, and polyhedral cages, among others) is still in its infancy, though some literature works seem to indicate a big potential. In addition, despite the ease of synthesizing ZnO structures, current research is still limited to laboratory-scale synthesis processes: industrial use would require these synthesis processes to be easily scalable to produce sufficient quantities to manufacture industrial piezo devices.

It seems reasonable to posit that interest in assessing the piezo-conversion efficiency of these different ZnO structures will continue to grow. This will undoubtedly promote the development of novel, reliable piezoelectric architectures that are durable and capable of effectively converting stray vibrations from crowded buildings, running vehicles, and human bodies into usable electrical energy.

Author contributions
D.D. and G.M. conceived the review work and equally drafted, reviewed, and edited the manuscript.

Funding
This work has not received funding.

Data availability
No datasets were generated or analysed during the current study.

Declarations

Ethics approval and consent to participate
Not applicable

Consent for publication
Not applicable.

Competing interests
The authors declare no competing interests.

Received: 27 June 2025 / Accepted: 5 November 2025
Published online: 02 February 2026

References

1. Vullers RJM, van Schaijk R, Doms I, Van Hoof C, Mertens R. Micropower energy harvesting. Solid State Electron. 2009;53:684–93.
2. Kamarudin SK, Daud WRW, Ho SL, Hasran UA. Overview on the challenges and developments of micro-direct methanol fuel cells (DMFC). J Power Sources. 2007;163:743–54.
3. Ferdous RMd, Reza AW, Siddiqui MF. Renewable energy harvesting for wireless sensors using passive RFID tag technology: A review. Renew Sust Energ Rev. 2016;58:1114–28.
4. Özgür Ü, Avrutin V, Morkoç H. Molecular beam epitaxy. Amsterdam: Elsevier; 2013.
5. Ali A, Shaukat H, Bibi S, Altabey WA, Noori M, Kouritem SA. Recent progress in energy harvesting systems for wearable technology. Energ Strat Rev. 2023;49:101124.
6. Sohail A, Ali A, Shaukat H, Bhatti FM, Ali S, Kouritem SA, et al. Integrating self-powered medical devices with advanced energy harvesting: A review. Energy Strat Rev. 2024;52:101328.
7. Abrahams SC, Bernstein JL. Remeasurement of the structure of hexagonal ZnO. Acta Crystallogr B. 1969;25:1233–6.
8. Shaukat H, Ali A, Bibi S, Altabey WA, Noori M, Kouritem SA. A Review of the recent advances in piezoelectric materials, energy harvester structures, and their applications in analytical chemistry. Appl Sci. 2023;13:1300.

9. Shaukat H, Ali A, Bibi S, Mehmood S, Altabey WA, Noori M, et al. Piezoelectric materials: Advanced applications in electrochemical processes. Energy Rep. 2023;9:4306–24.
10. Klingshirn C. ZnO: From basics towards applications. Phys Status Solidi (B). 2007;244:3027–73.
11. Ashrafi A, Jagadish C. Review of zincblende ZnO: Stability of metastable ZnO phases. J Appl Phys. 2007;102:071101.
12. Haider ST, Shah MA, Lee DG, Hur S. A review of the recent applications of aluminum nitride-based piezoelectric devices. IEEE Access. 2023;11:58779–95.
13. Mohammadpourfazeli S, Arash S, Ansari A, Yang S, Mallick K, Bagherzadeh R. Future prospects and recent developments of polyvinylidene fluoride (PVDF) piezoelectric polymer; fabrication methods, structure, and electro-mechanical properties. RSC Adv. 2023;13(1):370–87.
14. Sokolov PS, Baranov AN, Bell AMT, Solozhenko VL. Low-temperature thermal expansion of rock-salt ZnO. Solid State Commun. 2014;177:65–7.
15. Baranov AN, Sokolov PS, Tafeenko VA, Lathe C, Zubavichus YV, Veligzhanin AA, et al. Nanocrystallinity as a route to metastable phases: Rock salt ZnO. Chem Mater. 2013;25:1775–82.
16. Miao J, Liu B. Semiconductor Nanowires. Amsterdam: Elsevier; 2015.
17. Choi YS, Kang JW, Hwang DK, Park SJ. Recent advances in ZnO-based light-emitting diodes. IEEE Trans Electron Devices. 2010;57:26–41.
18. Jin C, Zhou J, Wu Z, Zhang JXJ. Doped Zinc Oxide-Based Piezoelectric Devices for Energy Harvesting and Sensing. Adv Energy Sustain Res. 2025;1:793–803.
19. Sezer N, Koç M. A comprehensive review on the state-of-the-art of piezoelectric energy harvesting. Nano Energy. 2021;80:105567.
20. Brusa E, Carrera A, Delprete C. A review of piezoelectric energy harvesting: Materials, design, and readout circuits. Actuators. 2023;12:457.
21. Ghazanfarian J, Mohammadi MM, Uchino K. Piezoelectric energy harvesting: a systematic review of reviews. Actuators. 2021;10:312.
22. He Q, Briscoe J. Piezoelectric energy harvester technologies: synthesis, mechanisms, and multifunctional applications. ACS Appl Mater Interfaces. 2024;16:29491–520.
23. Li S, Shan Y, Chen J, Chen X, Shi Z, Zhao L, et al. 3D printing and biomedical applications of piezoelectric composites: A critical review. Adv Mater Technol. 2025;10:2401160.
24. Han D, Song CK, Lee G, Song W, Park S. A comprehensive review of battery-integrated energy harvesting systems. Adv Mater Technol. 2024;9:2302236.
25. Baidya K, Roy A, Das K. A review of polymer-matrix piezoelectric composite coatings for energy harvesting and smart sensors. J Coat Technol Res. 2023;21:55–85.
26. Gołąbek J, Strankowski M. A review of recent advances in human-motion energy harvesting nanogenerators, self-powering smart sensors and self-charging electronics. Sensors. 2024;24:1069.
27. Khorsand Zak A, Yazdi ST, Abrishami ME, Hashim AM. A review on piezoelectric ceramics and nanostructures: fundamentals and fabrications. J Aust Ceram Soc. 2024;60:723–53.
28. Persano L, Camposeo A, Matino F, Wang R, Natarajan T, Li Q, et al. Advanced materials for energy harvesting and soft robotics: Emerging frontiers to enhance piezoelectric performance and functionality. Adv Mater. 2024;36:2405363.
29. Jean F, Khan MU, Alazzam A, Mohammad B. Advancement in piezoelectric nanogenerators for acoustic energy harvesting. Microsyst & Nanoeng. 2024;10:197.
30. Cai X, Wang Y, Cao Y, Yang W, Xia T, Li W. Flexural-mode piezoelectric resonators: structure, performance, and emerging applications in physical sensing technology, micropower systems, and biomedicine. Sensors. 2024;24:3625.
31. Pan X, Wu Y, Wang Y, Zhou G, Cai H. Mechanical energy harvesting based on the piezoelectric materials: Recent advances and future perspectives. Chem Eng J. 2024;497:154249.
32. Yang D, Sun A, Pan Y, Wang K. Mechanical energy harvesting: Advancements in piezoelectric nanogenerators. Int J Electrochem Sci. 2024;19:100793.
33. Sahoo S, Deka N, Panday R, Boomishankar R. Metal-free small molecule-based piezoelectric energy harvesters. Chem Commun. 2024;60:11655–72.
34. Wakshume DG, Płaczek MŁ. Optimizing piezoelectric energy harvesting from mechanical vibration for electrical efficiency: a comprehensive review. Electronics. 2024;13:987.
35. Bhatnagar R, Yadav V, Kumar U, Carrasco MF. Piezoelectric energy harvesting: from fundamentals to advanced applications. Energy Technol. 2025;13(4):2401455.
36. Ali A, Iqbal S, Chen X. Recent advances in piezoelectric wearable energy harvesting based on human motion: Materials, design, and applications. Energy Strategy Rev. 2024;53:101422.
37. Chen X, Zhu Q, Jiang B, Li D, Song X, Huang L, et al. Research progress of wood and lignocellulose in sustainable piezoelectric systems. Nano Energy. 2024;126:109650.
38. Yadav D, Tyagi N, Yadav H, James A, Sareen N, Kapoor M, et al. Effect of various morphologies and dopants on piezoelectric and detection properties of ZnO at the nanoscale: a review. J Mater Sci. 2023;58:10576–99.
39. Ayana A, Hou F, Seidel J, Rajendra BV, Sharma P. Microstructural and piezoelectric properties of ZnO films. Mater Sci Semicond Process. 2022;146:106680.
40. Srikanth KS, Wazeer A, Mathiyalagan P, Vidya S, Rajput K, Kushwaha HS. Nanostructured Zinc Oxide. Amsterdam: Elsevier; 2023.
41. Bhadwal N, Ben Mrad R, Behdinan K. Review of zinc oxide piezoelectric nanogenerators: piezoelectric properties, composite structures and power output. Sensors. 2023;23:3859.
42. Pandey RK, Dutta J, Brahma S, Rao B, Liu CP. Review on ZnO-based piezotronics and piezoelectric nanogenerators: aspects of piezopotential and screening effect. J Phys Mater. 2021;4(4):044011.
43. Janotti A, Van De Walle CG. Fundamentals of zinc oxide as a semiconductor. Rep Prog Phys. 2009;72(12):126501.
44. Karpina VA, Lazorenko VI, Lashkarev CV, Dobrowolski VD, Kopylova LI, Baturin VA, et al. Zinc oxide–analogue of GaN with new perspective possibilities. Cryst Res Technol. 2004;39(11):980–92.
45. Sharma DK, Shukla S, Sharma K, Kumar V. A review on ZnO: fundamental properties and applications. Mater Today. 2022;49:3028–35.
46. Thomas DG. The exciton spectrum of zinc oxide. J Phys Chem Sol. 1960;15:86–96.

47. Burgiel JC, Chen YS, Vratny F, Smolinsky G. Refractive Indices of ZnO, ZnS, and Several Thin-Film Insulators. J Electrochem Soc. 1968;115:729–32.
48. Anwar M, Kayani ZN, Hassan A, Sagheer R, Riaz S, Naseem S. Analysis of the Nd dopant on optical, dielectric and biological properties of ZnO nanostructures. J Mech Behav Biomed Mater. 2022;126:105016.
49. Narayanan PM, Wilson WS, Abraham AT, Sevanan M. Synthesis, characterization, and antimicrobial activity of zinc oxide nanoparticles against human pathogens. Bionanoscience. 2012;2:329–35.
50. Janaki AC, Sailatha E, Gunasekaran S. Synthesis, characteristics and antimicrobial activity of ZnO nanoparticles. Spectrochim Acta A Mol Biomol Spectrosc. 2015;144:17–22.
51. Saravanan R, Karthikeyan N, Gupta VK, Thirumal E, Thangadurai P, Narayanan V, et al. ZnO/Ag nanocomposite: an efficient catalyst for degradation studies of textile effluents under visible light. Mater Sci Eng C. 2013;33:2235–44.
52. Cauda V, Stassi S, Lamberti A, Morello M, Pirri CF, Canavese G. Leveraging ZnO morphologies in piezoelectric composites for mechanical energy harvesting. Nano Energy. 2015;18:212–21.
53. King DS, Nix RM. Thermal stability and reducibility of ZnO and Cu/ZnO catalysts. J Catal. 1996;160:76–83.
54. Nour ES, Nur O, Willander M. Zinc oxide piezoelectric nano-generators for low frequency applications. Semicond Sci Technol. 2017;32:064005.
55. Duraccio D, Capra PP, Malucelli G. UV-curable coatings for energy harvesting applications: Current state-of-the-art and future perspectives. Micro Nano Eng. 2024;23:100266.
56. Malucelli G, Fioravanti A, Francioso L, De Pascali C, Signore MA, Carotta MC, et al. Preparation and characterization of UV-cured composite films containing ZnO nanostructures: Effect of filler geometric features on piezoelectric response. Prog Org Coat. 2017;109:45–54.
57. Zhang T, Dong W, Keeter-Brewer M, Konar S, Njabon RN, Tian ZR. Site-specific nucleation and growth kinetics in hierarchical nanosyntheses of branched ZnO crystallites. J Am Chem Soc. 2006;128:10960–8.
58. Goel S, Kumar B. A review on piezo-/ferro-electric properties of morphologically diverse ZnO nanostructures. J Alloy Compd. 2020;816:152491.
59. Jang ES, Won J-H, Hwang S-J, Choy J-H. Fine tuning of the face orientation of ZnO crystals to optimize their photocatalytic activity. Adv Mater. 2006;18:3309–12.
60. Kong XY, Wang ZL. Spontaneous polarization-induced nanohelixes, nanosprings, and nanorings of piezoelectric nanobelts. Nano Lett. 2003;3:1625–31.
61. Wang ZL. ZnO nanowire and nanobelt platform for nanotechnology. Mater Sci Eng. 2009;64:33–71.
62. Li P, Liu H, Zhang Y-F, Wei Y, Wang X-K. Synthesis of flower-like ZnO microstructures via a simple solution route. Mater Chem Phys. 2007;106:63–9.
63. Zhang N, Yi R, Shi R, Gao G, Chen G, Liu X. Novel rose-like ZnO nanoflowers synthesized by chemical vapor deposition. Mater Lett. 2009;63:496–9.
64. Alenezi MR. Hierarchical zinc oxide nanorings with superior sensing properties. Mater Sci Eng. 2018;236–237:132–8.
65. Ong CB, Ng LY, Mohammad AW. A review of ZnO nanoparticles as solar photocatalysts: Synthesis, mechanisms and applications. Renew Sust Energ Rev. 2018;81:536–51.
66. Kumar R, Kumar G, Umar A. Pulse laser deposited nanostructured ZnO thin films: a review. J Nanosci Nanotechnol. 2014;14:1911–30.
67. Mohammed R, Ahmed S, Abdulrahman A, Hamad S. Synthesis and characterizations of ZnO thin films grown by physical vapor deposition technique. J Appl Sci Technol Trends. 2020;1:135–9.
68. Wang L, Zhang X, Zhao S, Zhou G, Zhou Y, Qi J. Synthesis of well-aligned ZnO nanowires by simple physical vapor deposition on c-oriented ZnO thin films without catalysts or additives. Appl Phys Lett. 2005;86:024108.
69. Zheng JH, Jiang Q, Lian JS. Synthesis and optical properties of flower-like ZnO nanorods by thermal evaporation method. Appl Surf Sci. 2011;257:5083–7.
70. Wu J-J, Liu S-C. Low-temperature growth of well-aligned ZnO nanorods by chemical vapor deposition. Adv Mater. 2002;14:215–8.
71. Tan ST, Chen BJ, Sun XW, Hu X, Zhang XH, Chua SJ. Properties of polycrystalline ZnO thin films by metal organic chemical vapor deposition. J Cryst Growth. 2005;281:571–6.
72. Shishodia PK, Kim HJ, Wakahara A, Yoshida A, Shishodia G, Mehra RM. Plasma enhanced chemical vapor deposition of ZnO thin films. J Non Cryst Solids. 2006;352:2343–6.
73. Armelao L, Fabrizio M, Gialanella S, Zordan F. Sol–gel synthesis and characterisation of ZnO-based nanosystems. Thin Solid Films. 2001;394:89–95.
74. Alias SS, Mohamad AA. Synthesis of Zinc Oxide by Sol-Gel Method for Photoelectrochemical Cells. Singapore: Springer; 2014.
75. Harun K, Hussain F, Purwanto A, Sahraoui B, Zawadzka A, Mohamad AA. ol–gel synthesized ZnO for optoelectronics applications: a characterization review. Mater Res Express. 2017;4:122001.
76. Arya S, Mahajan P, Mahajan S, Khosla A, Datt R, Gupta V, et al. Influence of processing parameters to control morphology and optical properties of Sol-Gel synthesized ZnO nanoparticles. ECS J Solid State Sci Technol. 2021;10:023002.
77. ElFaham MM, Mostafa AM, Mwafy EA. The effect of reaction temperature on structural, optical and electrical properties of tunable ZnO nanoparticles synthesized by hydrothermal method. J Phys Chem Solids. 2021;154:110089.
78. Sepulveda-Guzman S, Reeja-Jayan B, de la Rosa E, Torres-Castro A, Gonzalez-Gonzalez V, Jose-Yacaman M. Synthesis of assembled ZnO structures by precipitation method in aqueous media. Mater Chem Phys. 2009;115:172–8.
79. Baharudin KB, Abdullah N, Derawi D. Effect of calcination temperature on the physicochemical properties of zinc oxide nanoparticles synthesized by coprecipitation. Mater Res Express. 2018;5:125018.
80. Baruah S, Dutta J. Hydrothermal growth of ZnO nanostructures. Sci Technol Adv Mater. 2009;10:013001.
81. Gersten B. Solvothermal synthesis of nanoparticles. Chemfiles. 2005;5:11–2.
82. Li X, He G, Xiao G, Liu H, Wang M. Synthesis and morphology control of ZnO nanostructures in microemulsions. J Colloid Interface Sci. 2009;333:465–73.
83. Yildirim ÖA, Durucan C. Synthesis of zinc oxide nanoparticles elaborated by microemulsion method. J Alloys Compd. 2010;506:944–9.
84. Lim SK, Hwang SH, Kim S, Park H. Preparation of ZnO nanorods by microemulsion synthesis and their application as a CO gas sensor. Sens Actuators B Chem. 2011;160:94–8.

85. Chieng BW, Loo YY. Synthesis of ZnO nanoparticles by modified polyol method. Mater Lett. 2012;73:78–82.
86. Alves TEP, Kolodziej C, Burda C, Franco A. Effect of particle shape and size on the morphology and optical properties of zinc oxide synthesized by the polyol method. Mater Des. 2018;146:125–33.
87. Promnopas W, Thongtem T, Thongtem S. Effect of microwave power on energy gap of ZnO nanoparticles synthesized by microwaving through aqueous solutions. Superlattices Microstruct. 2015;78:71–8.
88. Hasanpoor M, Aliofkhazraei M, Delavari H. Microwave-assisted synthesis of zinc oxide nanoparticles. Procedia Mater Sci. 2015;11:320–5.
89. Ghosh S, Majumder D, Sen A, Roy S. Facile sonochemical synthesis of zinc oxide nanoflakes at room temperature. Mater Lett. 2014;130:215–7.
90. Katepetch C, Rujiravanit R, Tamura H. Formation of nanocrystalline ZnO particles into bacterial cellulose pellicle by ultrasonic-assisted in situ synthesis. Cellulose. 2013;20:1275–92.
91. Ghafari E, Feng Y, Liu Y, Ferguson I, Lu N. nvestigating process-structure relations of ZnO nanofiber via electrospinning method. Compos B Eng. 2017;116:40–5.
92. Di Mauro A, Zimbone M, Fragalà ME, Impellizzeri G. Synthesis of ZnO nanofibers by the electrospinning process. Mater Sci Semicond Process. 2016;42:98–101.
93. Choi S-H, Ankonina G, Youn D-Y, Oh S-G, Hong J-M, Rothschild A, et al. Hollow ZnO nanofibers fabricated using electrospun polymer templates and their electronic transport properties. ACS Nano. 2009;3:2623–31.
94. Liao Y, Fukuda T, Kamata N, Tokunaga M. Diameter control of ultrathin zinc oxide nanofibers synthesized by electrospinning. Nanoscale Res Lett. 2014;9:267.
95. de Melo EF, Alves KGB, Junior SA, de Melo CP. Synthesis of fluorescent PVA/polypyrrole-ZnO nanofibers. J Mater Sci. 2013;48:3652–8.
96. Laurenti M, Garino N, Porro S, Fontana M, Gerbaldi C. Zinc oxide nanostructures by chemical vapour deposition as anodes for Li-ion batteries. J Alloys Compd. 2015;640:321–6.
97. Wan H, Ruda HE. A study of the growth mechanism of CVD-grown ZnO nanowires. J Mater Sci: Mater Electron. 2010;21:1014–9.
98. Castillo-Saenz JR, Nedev N, Valdez-Salas B, Martinez-Puente MA, Aguirre-Tostado FS, Mendivil-Palma MI, et al. Growth of ZnO thin films at low temperature by plasma-enhanced atomic layer deposition using H2O and O2 plasma oxidants. J Mater Sci: Mater Electron. 2021;32:20274–83.
99. Toprak A, Tigli O. Piezoelectric energy harvesting: State-of-the-art and challenges. Appl Phys Rev. 2014;1:031104.
100. Kim HS, Kim JH, Kim J. A review of piezoelectric energy harvesting based on vibration. Int J Precis Eng Manuf. 2011;12:1129–41.
101. Choudhary P, Bhargava L, Singh V, Choudhary M, Kumar Suhag A. A survey–energy harvesting sources and techniques for internet of things devices. Mater Today Proc. 2020;30:52–6.
102. Kim S, Vyas R, Bito J, Niotaki K, Collado A, Georgiadis A, et al. Ambient RF energy-harvesting technologies for self-sustainable standalone wireless sensor platforms. Proc IEEE. 2014;102:1649–66.
103. Sanislav T, Zeadally S, Mois GD, Folea SC. Wireless energy harvesting: Empirical results and practical considerations for Internet of Things. J Netw Comput Appl. 2018;121:149–58.
104. Karan SK, Maiti S, Agrawal AK, Das AK, Maitra A, Paria S, et al. Designing high energy conversion efficient bio-inspired vitamin assisted single-structured based self-powered piezoelectric/wind/acoustic multi-energy harvester with remarkable power density. Nano Energy. 2019;59:169–83.
105. Wang DW, Mo JL, Wang XF, Ouyang H, Zhou ZR. Experimental and numerical investigations of the piezoelectric energy harvesting via friction-induced vibration. Energy Convers Manag. 2018;171:1134–49.
106. Priya S. Advances in energy harvesting using low profile piezoelectric transducers. J Electroceram. 2007;19:167–84.
107. Matiko JW, Grabham NJ, Beeby SP, Tudor MJ. Review of the application of energy harvesting in buildings. Meas Sci Technol. 2013;25:012002.
108. Liu H, Zhong J, Lee C, Lee S-W, Lin L. A comprehensive review on piezoelectric energy harvesting technology: Materials, mechanisms, and applications. Appl Phys Rev. 2018;5:041306.
109. Lee T, Lee W, Kim SW, Kim JJ, Kim BS. Flexible textile strain wireless sensor functionalized with hybrid carbon nanomaterials supported ZnO nanowires with controlled aspect ratio. Adv Funct Mater. 2016;26:6206–14.
110. Park T, Kim N, Kim D, Kim SW, Oh Y, Yoo JK, et al. An organic/inorganic nanocomposite of cellulose nanofibers and ZnO nanorods for highly sensitive, reliable, wireless, and wearable multifunctional sensor applications. ACS Appl Mater Interfaces. 2019;11:48239–48.
111. Young S-J, Tang W-L. Wireless zinc oxide based pH sensor system. J Electrochem Soc. 2019;166:B3047–50.
112. Wang ZL, Zhu G, Yang Y, Wang S, Pan C. Progress in nanogenerators for portable electronics. Mater Today. 2012;15:532–43.
113. Lee KY, Gupta MK, Kim SW. Transparent flexible stretchable piezoelectric and triboelectric nanogenerators for powering portable electronics. Nano Energy. 2015;14:139–60.
114. Lu A, Sun J, Jiang J, Wan Q. Low-voltage transparent electric-double-layer ZnO-based thin-film transistors for portable transparent electronics. Appl Phys Lett. 2010;96:043114.
115. Alagumalai A, Mahian O, Aghbashlo M, Tabatabaei M, Wongwises S, Wang ZL. Towards smart cities powered by nanogenerators: Bibliometric and machine learning–based analysis. Nano Energy. 2021;83:105844.
116. D. Polese, F. Maita, I. Lucarini, A. Ferraro, A. De Luca, D. Cannatà and L. Maiolo, A Wireless Sensor Network based on Laser-annealed ZnO Nanostructures for Advance Monitoring in Precise Agriculture, in SENSORNETS 2020 - Proceedings of the 9th International Conference on Sensor Networks (2020) pp. 177–181
117. N. Astan, D. Mohammadzamani, M. Gholami Parashkoohi and E. Ebrahimi, Energy harvesting and ANFIS modeling of a PVDF/GO-ZNO piezoelectric nanogenerator on a UAV, Open Agric 9, 20220275 (2024)
118. Bhaskaran PR, Rathnam JD, Koilmani S, Subramanian K. Multiresonant frequency piezoelectric energy harvesters integrated with high sensitivity piezoelectric accelerometer for bridge health monitoring applications. Smart Mater Res. 2017;2017:6084309.
119. Ahmad S, Abdul Mujeebu M, Farooqi MA. Energy harvesting from pavements and roadways: A comprehensive review of technologies, materials, and challenges. Int J Energy Res. 2019;43:1974–2015.
120. Zheng ZQ, Yao JD, Wang B, Yang GW. Light-controlling, flexible and transparent ethanol gas sensor based on ZnO nanoparticles for wearable devices. Sci Rep. 2015;5:11070.

121. Yuan M, Ma R, Ye Q, Bai X, Li H, Yan F, et al. Melt-stretched poly (vinylidene fluoride)/zinc oxide nanocomposite films with enhanced piezoelectricity by stress concentrations in piezoelectric domains for wearable electronics. Chem Eng J. 2023;455:140771.
122. Zhang Z, Chen Y, Guo J. ZnO nanorods patterned-textile using a novel hydrothermal method for sandwich structured-piezoelectric nanogenerator for human energy harvesting. Physica E Low Dimens Syst Nanostruct. 2019;105:212–8.
123. Lee KS, Shim J, Park M, Kim HY, Son DI. Transparent nanofiber textiles with intercalated ZnO@ graphene QD LEDs for wearable electronics. Compos B Eng. 2017;130:70–5.
124. Wu Y, Ma Y, Zheng H, Ramakrishna S. Piezoelectric materials for flexible and wearable electronics: A review. Mater & Des. 2021;211:110164.
125. Kahar K, Dhekekar R, Bhaiyya M, Balpande S, Kale P. MEMS based energy scavenger with interdigitated electrodes. Mater Today. 2023;72:350–60.
126. Mateu L, Moll F. Appropriate charge control of the storage capacitor in a piezoelectric energy harvesting device for discontinuous load operation. Sens Actuators A Phys. 2006;132:302–10.
127. Mahanty B, Ghosh SK, Jana S, Mallick Z, Sarkar S, Mandal D. ZnO nanoparticle confined stress amplified all-fiber piezoelectric nanogenerator for self-powered healthcare monitoring. Sustain Energy Fuels. 2021;5:4389–400.
128. Wang Y, Yu Y, Wei X, Narita F. Self-powered wearable piezoelectric monitoring of human motion and physiological signals for the postpandemic era: a review. Adv Mater Technol. 2022;7:2200318.
129. Kim MJ, Song Z, Yun TG, Kang MJ, Son DH, Pyun JC. Wearable fabric-based ZnO nanogenerator for biomechanical and biothermal monitoring. Biosens Bioelectron. 2023;242:115739.
130. Li M, Yao R, Liu Y. A flexible and ultra-highly sensitive tactile sensor based on Mg-doped ZnO nanorods for human vital signs and activity monitoring. Semicond Sci Technol. 2023;38:095012.
131. Yang T, Pan H, Tian G, Zhang B, Xiong D, Gao Y, et al. Hierarchically structured PVDF/ZnO core-shell nanofibers for self-powered physiological monitoring electronics. Nano Energy. 2020;72:104706.
132. Kim H, Yun S, Kim K, Kim W, Ryu J, Nam HG, et al. Breaking the elastic limit of piezoelectric ceramics using nanostructures: A case study using ZnO. Nano Energy. 2020;78:105259.
133. Abu Ali T, Pilz J, Schäffner P, Kratzer M, Teichert C, Stadlober B, et al. Piezoelectric properties of zinc oxide thin films grown by plasma-enhanced atomic layer deposition. Phys status solidi. 2020;217:2000319.
134. Synhaivskyi O, Albertini D, Gaffuri P, Chauveau J-M, Consonni V, Gautier B, et al. Evidence of piezoelectric potential and screening effect in single highly doped ZnO: Ga and ZnO: Al nanowires by advanced scanning probe microscopy. J Phys Chem C. 2021;125:15373–83.
135. Liu S, Han M, Feng X, Yu Q, Gu L, Wang L, et al. Statistical piezotronic effect in nanocrystal bulk by anisotropic geometry control. Adv Funct Mater. 2021;31:2010339.
136. Polewczyk V, Magrin Maffei R, Vinai G, Lo Cicero M, Prato S, Capaldo P, et al. ZnO thin films growth optimization for piezoelectric application. Sensors. 2021;21:6114.
137. Wang B, Zhang Q, He J, Huang F, Li C, Wang M. Co-catalyst-free large ZnO single crystal for high-efficiency piezocatalytic hydrogen evolution from pure water. J Energy Chem. 2022;65:304–11.
138. Nikolaev AL, Kazmina MA, Lyanguzov NV, Abdulvakhidov KG, Kaidashev EM. Synthesis of ZnO nanorods for piezoelectric resonators and sensors. J Adv Dielectr. 2022;12:2160020.
139. Golovanov E, Kolesov V, Anisimkin V, Osipenko V, Kuznetsova I. ZnO piezoelectric films for acoustoelectronic and microenergetic applications. Coatings. 2022;12:709.
140. Tran K, Tawfik SA, Spencer MJS. Restoring piezoelectric properties in 2D zinc oxide nanosheets by surface modifications: Implications for piezoelectric nanogenerators. ACS Appl Nano Mater. 2023;6:14767–76.
141. Yu Z, Bi J, Huang D, Zhao X, He Y. Readout circuit for a ZnO bulk-acoustic-wave X-ray dose rate detector. Nucl Instrum Methods Phys Res A. 2024;1067:169735.
142. Root SE, Savagatrup S, Printz AD, Rodriquez D, Lipomi DJ. Mechanical properties of organic semiconductors for stretchable, highly flexible, and mechanically robust electronics. Chem Rev. 2017;117:6467–99.
143. Mahapatra A, Ajimsha RS, Ittoop MO, Sharma A, Karmakar S, Shaikh A, et al. Flexible ZnO: PVDF based free standing piezoelectric nanogenerator for vibrational energy harvesting and wearable shoe insole pedometer sensor. J Alloys Compd. 2023;960:170898.
144. Li J, Zhao C, Xia K, Liu X, Li D, Han J. Enhanced piezoelectric output of the PVDF-TrFE/ZnO flexible piezoelectric nanogenerator by surface modification. Appl Surf Sci. 2019;463:626–34.
145. Habib M, Lantgios I, Hornbostel K. A review of ceramic, polymer and composite piezoelectric materials. J Phys D Appl Phys. 2022;55:423002.
146. Tan DDQ. The search for enhanced dielectric strength of polymer-based dielectrics: a focused review on polymer nanocomposites. J Appl Polym Sci. 2020;137:49379.
147. Vallem V, Sargolzaeiaval Y, Ozturk M, Lai Y, Dickey MD. Energy harvesting and storage with soft and stretchable materials. Adv Mater. 2021;33:2004832.
148. Eltouby P, Shyha I, Li C, Khaliq J. Factors affecting the piezoelectric performance of ceramic-polymer composites: A comprehensive review. Ceram Int. 2021;47:17813–25.
149. AlHamaydeh M, Ghazal Aswad N. Structural health monitoring techniques and technologies for large-scale structures: Challenges, limitations, and recommendations. Pract Period Struct Des Constr. 2022;27:03122004.
150. Jeronimo K, Koutsos V, Cheung R, Mastropaolo E. PDMS-ZnO piezoelectric nanocomposites for pressure sensors. Sensors. 2021;21:5873.
151. Zhang X, Le M-Q, Zahhaf O, Capsal J-F, Cottinet P-J, Petit L. Enhancing dielectric and piezoelectric properties of micro-ZnO/PDMS composite-based dielectrophoresis. Mater Des. 2020;192:108783.
152. Prashanthi K, Miriyala N, Gaikwad RD, Moussa W, Rao VR, Thundat T. Vibtrational energy harvesting using photo-patternable piezoelectric nanocomposite cantilevers. Nano Energy. 2013;2:923–32.
153. Mata A, Fleischman AJ, Roy S. Characterization of polydimethylsiloxane (PDMS) properties for biomedical micro/nanosystems. Biomed Microdevices. 2005;7:281–93.
154. Lötters JC, Olthuis W, Veltink PH, Bergveld P. The mechanical properties of the rubber elastic polymer polydimethylsiloxane for sensor applications. J Micromech Microeng. 1997;7:145–7.

155. Beigh NT, Mallick D. Low-cost, high-performance piezoelectric nanocomposite for mechanical energy harvesting. IEEE Sens J. 2021;21:21268–76.
156. Kandpal M, Sharan C, Poddar P, Prashanthi K, Apte PR, Ramgopal Rao V. Photopatternable nano-composite (SU-8/ZnO) thin films for piezo-electric applications. Appl Phys Lett. 2012;101:104102.
157. Krishna B, Chaturvedi A, Mishra N, Das K. Nanomechanical characterization of SU8/ZnO nanocomposite films for applications in energy-harvesting microsystems. J Micromech Microeng. 2018;28:115013.
158. Duraccio D, Capra PP, Fioravanti A, Malucelli G. Influence of mechanical properties on the piezoelectric response of UV-cured composite films containing different ZnO morphologies. Polymers. 2023;15:1159.
159. M. A. Signore, G. Malucelli, D. Duraccio, C. De Pascali, A. Fioravanti, P. Siciliano and L. Francioso, Synthesis and Piezoelectric Characterization of UV-Curable Nanocellulose/ZnO/AlN Polymeric Flexible Films for Green Energy Generation Applications, Proceedings 56, 36 (2020)
160. Singh HH, Singh S, Khare N. Enhanced β-phase in PVDF polymer nanocomposite and its application for nanogenerator. Polym Adv Technol. 2018;29:143–50.
161. Sorayani Bafqi MS, Bagherzadeh R, Latifi M. Fabrication of composite PVDF-ZnO nanofiber mats by electrospinning for energy scavenging application with enhanced efficiency. J Polym Res. 2015;22:130.
162. Thakur P, Kool A, Hoque NA, Bagchi B, Khatun F, Biswas P, et al. Superior performances of in situ synthesized ZnO/PVDF thin film based self-poled piezoelectric nanogenerator and self-charged photo-power bank with high durability. Nano Energy. 2018;44:456–67.
163. Yi J, Song Y, Cao Z, Li C, Xiong C. Gram-scale Y-doped ZnO and PVDF electrospun film for piezoelectric nanogenerators. Compos Sci Technol. 2021;215:109011.
164. Shee C, Banerjee S, Bairagi S, Baburaj A, Naveen KS, Aliyana AK, et al. A critical review on polyvinylidene fluoride (PVDF)/zinc oxide (ZnO)-based piezoelectric and triboelectric nanogenerators. J Phys. 2024;6:032001.
165. Guo D, Zeng F, Dkhil B. Ferroelectric polymer nanostructures: fabrication, structural characteristics and performance under confinement. J Nanosci Nanotechnol. 2014;14:2086–100.
166. Thomann H. Piezoelectric ceramics. Adv Mater. 1990;2(10):458–63.
167. Vedhanarayanan B, Lakshmi KCS, Lin T-W. Interfacial tuning of polymeric composite materials for high-performance energy devices. Batteries. 2023;9(10):487.
168. Narasimulu AA, Zhao P, Soin N, Prashanthi K, Ding P, Chen J, et al. Significant triboelectric enhancement using interfacial piezoelectric ZnO nanosheet layer. Nano Energy. 2017;40:471–80.
169. Mahapatra A, Ajimsha RS, Misra P. Self-powered high responsivity ultraviolet radiation sensor by coupling ZnO based piezoelectric nanogenerator and photodetector. Appl Phys Lett. 2024;124:103503.
170. Kaur G, Sharma AK, Jassal M, Agrawal AK. ZnO-poly (acrylonitrile) composite films with improved piezoelectric properties for energy harvesting and sensing applicationsCompos. Sci Technol. 2023;243:110260.
171. Wang ZY, Su KH, Fan HQ, Wen ZY. Possible reasons that piezoelectricity has not been found in bulk polymer of polyvinylidene cyanide. Polymer. 2008;49:2542–7.
172. Zhu Q, Song X, Chen X, Li D, Tang X, Chen J, et al. A high performance nanocellulose-PVDF based piezoelectric nanogenerator based on the highly active CNF@ ZnO via electrospinning technology. Nano Energy. 2024;127:109741.
173. Motora KG, Wu C-M, Rani GM, Yen W-T, Lin K-S. Effect of electrode patterns on piezoelectric energy harvesting property of zinc oxide polyvinylidene fluoride based piezoelectric nanogenerator. Renew Energy. 2023;217:119208.
174. Rahsepar H, Hayati R, Javapour S. Evaluation of the dielectric, and piezoelectric properties and optimizing the figure of merit of the 0–3 KNN-08 ZnO/PVDF-HFP piezoelectric composite by the Taguchi method. J Alloy Compd. 2024;1006:176373.
175. Moezzi M, Bakhtari K, Ranjbar-Mohammadi M, Kamali Moghaddam M, Barez F. Fabrication and characterization of piezoelectric poly (lactic acid)/ZnO bionanocomposite films. Polym Bull. 2025;82(10):4423–42.
176. Huang Y, Chen S, Li Y, Lin Q, Wu Y, Shi Q. Flexible piezoelectric sensor based on PAN/MXene/PDA@ ZnO composite film for human health and motion detection with fast response and highly sensitive. Chem Eng J. 2024;488:150997.
177. Wang H, Xia H, Yang W, Xu Z, Natsuki T, Ni Q-Q. ZnO nanoparticles and carboxylated MWNTs multi-networks composite hydrogels with piezoelectric properties and human motion sensing. Diam Relat Mater. 2024;142:110782.
178. Misra M, Srivastava AK, Kadam AN, Salunkhe TT, Kumar V, Nikalje APG. Substantial enhancement of optoelectronics and piezoelectric properties of novel hollow ZnO nanorods towards efficient flexible touch and bending sensor. Colloids Surf A. 2024;685:133232.
179. Taleb S, van Lingen WM, Acuautla M. Toward high quality tactile sensors using ZnO/P (VDF-TrFE) flexible piezoelectric composite films. Mater Adv. 2024;5:7671–8.
180. Wang J, Liu S, Zhang X, Hou Y, Liu Y, Li X, et al. High-performance piezoelectric nanogenerators with P (VDF-TrFE)/AlN/ZnO nanofiber membranes for harvesting and monitoring gesture movements. Chem Eng J. 2025;510:161818.
181. He P, Li J, Zhang B, Huang L, Zhong Y, Li S, et al. Mechanically robust porous polyimide films for piezoelectric sensing at extreme condition. Compos Sci Technol. 2025;261:111006.
182. Fernández-Gil F, Olate-Moya F, Aguilar-Cosme JR, García-Molleja J, Fernández-Blázquez JP, Cartmell S, et al. Micro-arranged ZnO particles and conductive fillers in PCL composites for enhanced piezoelectric and dielectric properties in bone tissue engineering applications. Mater Des. 2025;251:113672.
183. Ayoub I, Kumar V, Abolhassani R, Sehgal R, Sharma V, Sehgal R, et al. Advances in ZnO: Manipulation of defects for enhancing their technological potentials. Nanotechnol Rev. 2022;11(1):575–619.
184. Mahapatra A, Ajimsha RS, Misra P. Oxygen annealing induced enhancement in output characteristics of ZnO based flexible piezoelectric nanogenerators. J Alloy Compd. 2022;913:165277.
185. Gui D, Gao Y, Mi X, Yao B, Zhang Z, Xu Y, et al. Advancements in enhancement strategies for piezoelectric nanogenerator output performance and their applications in self-powered sensors. ACS Sens. 2025;10(9):6292–315.
186. Desai AV, Haque MA. Mechanical properties of ZnO nanowires. Sens Actuators, A. 2007;134(1):169–76.
187. Raha S, Ahmaruzzaman M. ZnO nanostructured materials and their potential applications: progress, challenges and perspectives. Nanoscale advances. 2022;4(8):1868–925.
188. Minami T, Miyata T, Ohtani Y, Kuboi T. Effect of thickness on the stability of transparent conducting impurity-doped ZnO thin films in a high humidity environment. Rapid Res Lett. 2006;1:1.

189. Wu NP, Zhang NJ, Lu NJ, Li NX, Wu NC, Sun NR, et al. Instability induced by ultraviolet light in ZnO thin-film transistors. IEEE Trans Electron Devices. 2014;61(5):1431–5.
190. Domenech J, Prieto A. Stability of zinc oxide particles in aqueous suspensions under UV illumination. J Phys Chem. 1986;90(6):1123–6.
191. Illiberi A, Scherpenborg R, Theelen M, Poodt P, Roozeboom F. On the environmental stability of ZnO thin films by spatial atomic layer deposition. J Vacuum Sci Technol A. 2013;31:6.
192. Djurišić AB, Chen X, Leung YH, Ng AMC. ZnO nanostructures: growth, properties and applications. J Mater Chem. 2012;22(14):6526–35.
193. Hu J, Dong M. Recent advances in two-dimensional nanomaterials for sustainable wearable electronic devices. J Nanobiotechnol. 2024;22(1):63.
194. Cao S, Zou H, Jiang B, Li M, Yuan Q. Incorporation of ZnO encapsulated MoS_2 to fabricate flexible piezoelectric nanogenerator and sensor. Nano Energy. 2022;102:107635.
195. Kamlesh K, Dhekekar R, Bhaiyya M, Srivastava SK, Rewatkar P, Balpande S, et al. Optimization of MEMS-based Energy Scavengers and output prediction with machine learning and synthetic data approach. Sens Actuators, A. 2023;358:114429.
196. Gotte M, Rama Sreekanth PS. ntegrating artificial intelligence with piezoelectric nanogenerators: a review on advancements in smart energy harvesting technologies. J Mater Sci. 2025;1:1–32.
197. G. Al Zohbi, Revolutionizing Energy Harvesting: Integrating AI with Ambient Energy Sources. Available at SSRN 5412928.

Publisher's Note

Springer Nature remains neutral with regard to jurisdictional claims in published maps and institutional affiliations.